

# Near-infrared photometry of Galactic planetary nebulae with the VVV Survey

W. A. Weidmann<sup>1,★</sup>, R. Gamen<sup>2,★★</sup>, P.A.M. van Hoof<sup>3</sup>, A. Zijlstra<sup>4</sup>, D. Minniti<sup>5,6,7</sup> and M. G. Volpe<sup>8</sup>

<sup>1</sup> Observatorio Astronómico Córdoba, Universidad Nacional de Córdoba, Argentina  
e-mail: walter@mail.oac.uncor.edu

<sup>2</sup> Instituto de Astrofísica de La Plata, CCT La Plata-CONICET, Universidad Nacional de La Plata, Argentina  
e-mail: rgamen@fcaglp.unlp.edu.ar

<sup>3</sup> Royal Observatory of Belgium, Ringlaan 3, 1180 Brussels, Belgium

<sup>4</sup> Jodrell Bank Centre for Astrophysics, University of Manchester, Manchester M13 9PL, UK

<sup>5</sup> Departamento de Astronomía y Astrofísica, Pontificia Universidad Católica de Chile, Av. Vicuña Mackenna 4860, Casilla 306, Santiago 22, Chile  
e-mail: dante@astro.puc.cl

<sup>6</sup> Vatican Observatory, V00120 Vatican City State, Italy

<sup>7</sup> Departamento de Ciencia Fisicas, Universidad Andres Bello, Santiago, Chile

<sup>8</sup> Instituto de Astronomía Teórica y Experimental, Argentina

Preprint online version: September 11, 2018

## ABSTRACT

**Context.** Planetary nebulae (PNe) are powerful tracers of evolved stellar populations. Among the 3000 known PNe in the Galaxy, about 600 are located within the 520 square-degree area covered by the VVV survey. The VVV photometric catalogue provides an important new dataset for the study of PNe, with high-resolution imaging in five near-infrared bands.

**Aims.** There are various colour-colour diagrams that can be obtained from the VVV filters. We investigate the location of PNe in these diagrams and the separation from other types of objects. This includes the new  $Y-J$  vs.  $Z-Y$  diagram.

**Methods.** Aperture photometry of known PNe in the VVV area was retrieved from source catalogues. Care was taken to minimise any confusion with field stars. The colours of the PNe we are determined for  $(H-K_s)$ ,  $(J-H)$ ,  $(Z-Y)$ , and  $(Y-J)$ , and compared to stars and to other types of emission line objects. Cloudy photo-ionisation models were used to predict colours for typical PNe.

**Results.** We present near-infrared photometry for 353 known PNe. The best separation from other objects is obtained in the  $(H-K_s)$  vs.  $(J-H)$  diagram. We calculated the emission-line contribution to the in-band flux based on a model for NGC 6720: we find that this is highest in the Z and Y bands at over 50%, lower in the J band at 40%, and lowest in the H and Ks bands at 20%. A new view of PNe in the wavelength domain of the Z and Y bands is shown. Photo-ionisation models are used to explore the observed colours in these bands. The Y band is shown to be dominated by He I  $1.083\mu\text{m}$  and He II  $1.012\mu\text{m}$ , and colours involving this band are very sensitive to the temperature of the ionizing star.

**Conclusions.** The VVV survey represents a unique dataset for studying crowded and obscured regions in the Galactic plane. The diagnostic diagrams presented here allow one to study the properties of known PNe and to uncover objects not previously classified.

**Key words.** planetary nebulae: general – infrared: ISM – catalogues

## 1. Introduction

Planetary nebulae (PNe) are luminous and short-lived products of evolved low-mass stars ( $0.8M_\odot < M < 8M_\odot$ ). The stars eject much of their envelopes during a phase of strong mass loss at the end of the asymptotic giant branch (AGB). The ejecta become ionised after a brief transition phase, when the star rapidly increases in temperature, the ionised ejecta form a visible planetary nebula. The ejected material is enriched in a variety of elements (He, C, N, O, Ne, Mg, s-process elements), through nuclear burning and dredge-up during the AGB phase. The transfer of this gas to the interstellar medium affects the overall chemical evolution of the Galaxy. PNe also provide information about the recent star-forming history in our Galaxy (e.g. Maciel & Costa 2003). Thus, PNe are key objects in the study of stellar and galactic evolution.

The distribution of known Galactic PNe shows a lack of objects within the Galactic plane and towards the central regions of the Galaxy (e.g. Miszalski et al. 2008, Fig. 6c). This is caused by high extinction and by severe crowding. To obtain a better understanding of the whole Galactic PN population, deeper surveys are needed in these regions. Near-infrared (NIR) observations provide an important tool, because they are less affected by extinction and benefit from better seeing.

The NIR fluxes of PNe depend on a broad range of emission mechanisms, including warm dust continuum emission, ionic and atomic permitted and forbidden line transitions, and the underlying free-free and bound-free components of gaseous continuum emission. Continuum emission from cool stellar companions, or the PN central star itself, may also contribute. Broad band IR photometry of galactic PNe has been reported in the literature by several authors (e.g. Allen 1973; Whitelock 1985; Pena & Torres-Peimbert 1987; Garcia-Lario et al. 1997). The complete and homogeneous 2MASS survey has sub-

\* Member of Carrera del Investigador CONICET, Argentina.

\*\* Member of Carrera del Investigador CONICET, Argentina.

stantially increased the number of PNe with NIR observations (Ramos-Larios & Phillips 2005; Phillips & Zepeda-García 2009), but was limited by its 4-arcsec spatial resolution. The VISTA Variables in the Via Lactea (VVV<sup>1</sup>) public survey now provides deeper and higher resolution observational data, and will greatly improve the number of PNe observations in extinted and/or crowded regions of the sky (Minniti et al. 2010).

The past studies of PNe have used the *JHK* bands. The VVV survey adds two original bands, the *Z* and *Y* bands<sup>2</sup>. Therefore, our motivations are to improve the infrared photometry of PNe in order to contribute to the knowledge of stellar evolution, and to generate tools for characterising the NIR flux of PNe.

## 2. The VVV observational database

The VISTA 4.1m telescope at the Paranal Observatory (Emerson & Sutherland 2010) is equipped with the instrument VIRCAM (VISTA InfraRed CAMera; Emerson et al. 2006; Dalton et al. 2006). The camera contains 16 near infrared detectors, of  $2048 \times 2048$  pixels each. The pixel size corresponds to 0.34 arcsec on the sky. There are gaps between the detectors so that a single exposure gives a non-contiguous sky coverage. Such a single exposure is called a pawprint. By combining 6 *pawprints* with appropriate offsets, a contiguous coverage of a field is achieved, where all pixels (apart from those at the edges) have at least two independent exposures. In the VISTA terminology such a field is called a *tile*; it covers a 1.64 square deg field of view, 1.5 square deg of which is covered by at least 2 pawprints.

The data reduction was carried out in the typical manner for infrared imaging. Details of the procedure are described in Irwin et al. (2004). The median image quality measured on the reduced VVV tile images is around 0.8'' for  $K_s$ , 0.9'' for the *J* band, and up to 1.0'' for the *Z*-band.

The data calibration is performed by the VISTA Data Flow System (VDFS) pipeline at the Cambridge Astronomy Survey Unit (CASU). The photometry is tied to unsaturated 2MASS stars present in the VVV images, even for the *Z* and *Y* filters (not observed by 2MASS), for which colour equations are applied<sup>3</sup>. For more detail about photometric calibration see Gonzalez et al. (2011) for all 5 filters.

In this paper we use the magnitudes from the first data release of the VVV Survey (Saito & et al. 2012). The VISTA Science Archive<sup>4</sup> provides two different catalogues, *vvvDetection* and *vvvSource*. The first one contains the individual detections for sources originating from multiframe images taken from the VVV. The second one lists the merged sources (in the five bands) from detections in *vvvDetection* catalogue (Saito & et al. 2012). In our catalogue, we used the Source-table, with a 2.8'' aperture diameter.

The catalogue contains a flag to indicate the most probable morphological classification, in particular “-1” is used to denote stellar objects, “-2” borderline stellar, “0” is noise, and “1” is used for non-stellar objects. There are also further flags: “-7”, denoting sources containing bad pixels, and the flag “-9” is used for saturated stars (Irwin et al. 2004). This makes it possible to

reject some bad measurements and to identify extended emission sources.

Objects with  $J < 11.8$ ,  $H < 11.0$ , or  $K_s < 11.0$  are saturated. We considered  $ZY < 12.5$  to indicate saturation, taking into account that the magnitudes in these two bands are probably not as well calibrated as those at *JHK*<sub>s</sub> due to the extrapolation needed. The magnitudes at which saturation occurs are dependent on the fields, partly because of seeing, and partly because there are some differences in exposure times between the bulge ( $-10^\circ < l < 10^\circ$  and  $-10^\circ < b < 5^\circ$ ) and disc ( $-65^\circ < l < -10^\circ$  and  $-2^\circ < b < 2^\circ$ ). We prefer to adopt the limits shown above.

The magnitudes from the aperture photometry are extracted from the catalogues following the equation  $\text{mag} = \text{zp} - (\text{airm} - 1) \times C - 2.5 \times \log_{10}(F/T) - \text{AC}$ , where  $\text{zp}$ = photometric zero-point for default extinction,  $\text{airm}$  = air mass,  $C$ = default extinction in the passband,  $F$ = aperture flux,  $T$ = exposure times and  $\text{AC}$ = aperture correction in magnitudes.

We refer the reader to Saito & et al. (2012) for a description of the photometric errors in the *ZYJHK*<sub>s</sub> filters as a function of the magnitude at different levels of crowding along the VVV area<sup>5</sup>.

## 3. Sources of $0.8\text{-}2.1\mu\text{m}$ emission in planetary nebulae in the VVV filters

For a better understanding of the results shown in this paper it is worth studying the characteristics of the near infrared emission observed in PNe. Whitelock (1985) gave a complete description of the principal emission sources in the *J*, *H*, *K*<sub>s</sub> bands, thermal plasma continuum, thermal dust emission, hot stellar continuum, emission lines and cool stellar continuum from a companion. Their discussion is based on the SAAO filters which slightly differ from other systems. In particular, the SAAO *J*-band includes the strong HeI 1.083 micron line at 50% transmission, which can dominate the flux in that band. The VISTA (and 2MASS) *J*-band filter excludes this line and it marginally intrudes instead in the *Y*-filter.

In the new photometric bands *Z* and *Y*, the dust contribution is negligible. Emission from free-free (FF) and bound-free (BF) transitions is marginally weaker. The stellar continuum gains importance, however the major flux contribution comes from emission lines. The *Z* band is dominated by [S III] at  $0.9069\mu\text{m}$ , and the *Y* band by Pa $\delta$  and He II at  $1.0124\mu\text{m}$ . Figure 1 shows the *ZYJ* transmission curves, in comparison to the spectrum of IC 5117, a medium excitation-class planetary nebula.

The 2MASS *J* band is somewhat wider than the VISTA *J* band. But the dominant Pa $\beta$  is covered by both filters, whilst neither filter contains other significant emission lines. Therefore, we do not expect a major discrepancy between both magnitudes.

IPHAS (The INT/WFC Photometric H-alpha Survey, Drew et al. 2005), its southern extension VPHAS, and DENIS (Deep Near-Infrared Southern Sky Survey, Epchtein et al. 1997) contain two optical bands that overlap in some spectral range with the *Z* VISTA band: these are *i'* (centred at  $0.7743\mu\text{m}$ ) and *I* ( $0.8000\mu\text{m}$ ) respectively. However, magnitudes obtained from these optical bands cannot be compared with the *Z* one because the filters are too different.

To further test the emission mechanisms contributing to the VVV bands, we made use of the published photo-ionisation model of van Hoof et al. (2010) for NGC 6720, the Ring Nebula.

<sup>1</sup> <http://vvvsurvey.org/>

<sup>2</sup> We found only a single paper using the *Y* broad band (Miszalski et al. 2011).

<sup>3</sup> More details about VISTA data processing is available from <http://casu.ast.cam.ac.uk/surveys-projects/vista/data-processing>

<sup>4</sup> <http://horus.roe.ac.uk/vsa>

<sup>5</sup> Errors in the fluxes are based on Poissonian statistics. A comprehensive description is available at Cross et al. (2012)

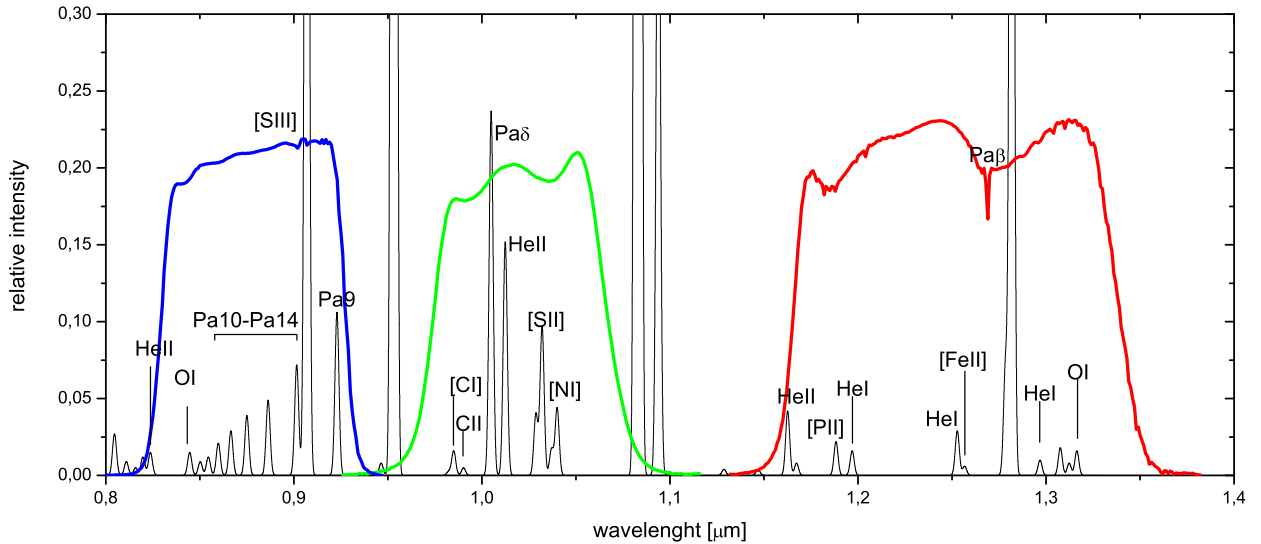


**Fig. 1.** Transmission curves for the  $Z$ ,  $Y$  and  $J$  broad-band filters (the effective wavelengths are  $0.878$ ,  $1.021$  and  $1.254\,\mu\text{m}$  respectively), the filters are multiplied by a model atmosphere. The spectrum of the PN IC 5117 is superimposed (Rudy et al. 2001), scaled to  $\text{Pa}\beta=1$ .

This is the archetypal planetary nebula; the nebula is bipolar, seen almost pole-on, optically thick to ionizing radiation except towards the poles. The Ring Nebula has a central star which has already entered the cooling track, and in response to the fading of the star parts of the outer nebula have begun to recombine. The photo-ionisation model uses as ionizing source a H-Ni model stellar atmosphere from Rauch (2003) with a temperature of  $T_{\text{eff}} = 135\,\text{kK}$ . The electron density of the model is  $n_e = 416\,\text{cm}^{-3}$ . For comparison, IC 5117 shown in Fig. 1 has  $T_{\text{eff}} = 120\,\text{kK}$  and density  $n_e = 9 \times 10^4\,\text{cm}^{-3}$  (Hyung et al. 2001). The model was calculated with version C10.00 of the Cloudy photo-ionisation code, last described by Ferland et al. (1998). The model incorporates the neutral region, to capture molecular hydrogen emission. We used this Cloudy model to calculate the free-free and bound-free continuum from both hydrogen and helium, and lines from ionised and neutral species, and from molecular hydrogen. The stellar continuum is also included but is not important at these long wavelengths and high stellar temperatures. The output model spectrum was convolved with the transmission curves from the VISTA filters combined with the telescope and instrument throughput and the detector sensitivity. Note that the model is for a nebula without interstellar reddening but does include a small amount of internal reddening.

Table 1 shows the detailed list of major lines which contribute to the in-band flux. The  $Z$  and  $J$ -bands are dominated by one line. The  $Y$  band also has one dominant line ( $\text{He I}$ ) but it is located at the edge of the transmission curve.  $H$  and  $K_s$  have a scattering of fainter lines. The total contribution of emission lines to the in-band flux is much higher for  $Y$  and  $Z$  than for the other three bands. The  $Z$  and  $Y$ -filters have a strong line close to the edge of the transmission curve, and small changes in the filter responses can have significant effects on the line contributions.

The specific line contributions will also depend on the excitation of the nebula especially for the  $Z$ -band.

## 4. Results

### 4.1. Description of the sample

There are 579 known PNe listed by Acker et al. (1992), Parker et al. (2006, MASH I), and Miszalski et al. (2008, MASH II) whose coordinates (Kerber et al., 2003) fall within the VVV area<sup>6</sup>.

We retrieved the processed and calibrated  $ZYJHK_s$  images (tiles) from the Cambridge Astronomical Survey Unit (CASU VIRCAM pipeline v1.1<sup>7</sup>; Irwin et al. 2004) and also retrieved the MASH  $\text{H}\alpha$  images (Parker et al. 2005). The planetary nebulae were identified from the  $\text{H}\alpha$  images using Kerber et al. (2003), the MASH catalogue and identification charts (Kinman et al. 1988; Beaulieu et al. 1999; Jacoby & Van de Steene 2004). We identified the related VVV source taking into account its symmetry with respect to the  $\text{H}\alpha$  emission. The visual examination was essential. Cross-correlation between the VVV and PNe catalogues (Kerber et al. 2003 for example) did not give satisfactory results for many sources. Therefore, the VVV sources were associated with the PNe by eye. Up to 82% of the sample are closer than 1.4 arcsec to the catalogue coordinates of Kerber et al. (2003).

From the initial sample of 579 PNe, 75 are highly extended sources and these will be considered in future papers, and 123 PNe could not be related to any source in the VVV images, perhaps because they have low surface brightness or the central star

<sup>6</sup> The IPHAS survey (Viironen et al. 2009a) does not overlap with the VVV area.

<sup>7</sup> Data release 1.1, <http://casu.ast.cam.ac.uk/surveys-projects/vista>

**Table 1.** Line contribution from the (unreddened) NGC 6720 model results. The columns give the element, wavelength, log flux in usual units, the line intensity relative to H $\beta$ , and the combined transmission of the sky, telescope, filter, and detector at this wavelength. Note that the model fluxes have not been multiplied with the transmission. The Z, Y and J bands are dominated by one line (but for the Y band it is located at the edge of the filter). H and K<sub>s</sub> have a scattering of fainter lines. The total contribution of emission lines to the in-band flux is also given. This is much higher for Y and Z than for the other three bands.

line	$\lambda$ [ $\mu\text{m}$ ]	flux [log erg cm $^{-2}$ s $^{-1}$ ]	$I(\text{line})/I(\text{H}\beta)$	transm.
<i>Z band (<math>0.878 \pm 0.097 \mu\text{m}</math>)</i>				
line contribution 55%				
[S III]	0.9069	-10.762	0.1591	0.717
H I	0.9229	-11.576	0.0244	0.644
H I	0.9015	-11.716	0.0177	0.712
H I	0.8863	-11.842	0.0132	0.707
H I	0.8750	-11.956	0.0102	0.698
[Cl II]	0.8579	-12.012	0.0089	0.677
<i>Y band (<math>1.021 \pm 0.093 \mu\text{m}</math>)</i>				
line contribution 55%				
He I	1.083	-10.342	0.4182	0.048
[C I]	0.985	-11.166	0.0627	0.597
H I	1.005	-11.236	0.0534	0.645
He II	1.012	-11.305	0.0456	0.669
[S II]	1.033	-11.382	0.0382	0.640
[N I]	1.040	-12.026	0.0087	0.645
<i>J band (<math>1.254 \pm 0.172 \mu\text{m}</math>)</i>				
line contribution 39%				
H I	1.282	-10.772	0.1555	0.680
He II	1.163	-12.026	0.0087	0.226
Fe II	1.257	-12.109	0.0072	0.730
He I	1.278	-12.135	0.0067	0.668
<i>H band (<math>1.646 \pm 0.291 \mu\text{m}</math>)</i>				
line contribution 21%				
H I	1.817	-11.890	0.0118	0.040
H I	1.736	-12.031	0.0086	0.843
H I	1.681	-12.158	0.0064	0.850
Fe II	1.644	-12.182	0.0061	0.825
<i>K<sub>s</sub> band (<math>2.149 \pm 0.309 \mu\text{m}</math>)</i>				
line contribution 22%				
H I	2.166	-11.549	0.0260	0.833
He I	2.058	-11.769	0.0156	0.616

**Notes.** Next to the band are indicated the effective wavelengths and the width of VISTA's filters.

is too weak in the NIR bands. The remaining PNe analysed in this paper are related to sources in the VVV catalogues with NIR emission mainly enclosed in an area of 1.4 arcsec of radius (even in PNe of high surface brightness and appreciable angular size); in this sense we are observing the emission from the central regions of the nebula. The integrated flux may be underestimated where the nebula is larger than the aperture used here. See Appendix A for a discussion about the used aperture.

In our catalogue we divide the data into five categories (see Table 3 and 5):

- Objects with photometric data (not necessarily in the five bands).
- NIR emission of the PN is detected in tile frames, but there are no photometric data in the VSA database (S/D).
- Extended objects, where the NIR emission is larger than 3'' in diameter (ext).

- PNe extended (in H $\alpha$ ) without NIR sources in the regions of their geometrical centre (N/D).
- Objects with unreliable photometry, i.e. large uncertainty in the magnitudes (>0.2), classified as noise or saturated by the pipeline (bad ph.).

Nearly 80% of the sample is detected in at least one band. Although the integration times in the region of the bulge are shorter than in the plane (4s and 10s per frame for the K<sub>s</sub> band), the percentage of objects not detected for the plane and bulge are comparable. We interpret this as that, on average, the bulge images show better contrast than the plane ones.

In general, extended PNe at H $\alpha$  are related to unresolved or small extended ( $\text{PSF}_{\text{PN}} \geq \text{PSF}_{\text{field}}$ ) sources in the NIR images. In these cases, it is probable that we are measuring the central star of the PN, or emission from its immediate environment. The coordinates are shown in Table 3.

Our catalogue (Table 3) includes 353 PNe with ZYJHK<sub>s</sub> photometrical data. From these, 209 are new NIR detections. The remaining ones were previously detected and measured by 2MASS, however the VVV photometry improves on these earlier determinations.

#### 4.2. Comparison between VVV and 2MASS

To compare the VVV magnitudes with those of 2MASS (The 2MASS Point Source catalogue) ones, we selected objects with  $J(2\text{MASS}) < 16.0$  and  $J(\text{VVV}) > 11.8$ ,  $H(2\text{MASS}) < 15.5$  and  $H(\text{VVV}) > 11.0$ ,  $K_s(2\text{MASS}) < 14.0$  and  $K_s(\text{VVV}) > 11.0$ , according to the upper and lower detection limit, respectively. The brightest objects in VVV were not taken into account since they are near the saturation limit. We also did not consider the weakest PNe in the 2MASS survey because of the uncertainties on the photometry.

The 2MASS Point Source Catalogue was constructed using aperture photometry with 4'' radius (Skrutskie et al. 2006), while we used aperture photometry with a 1.41'' radius. The difference between both magnitudes is about 0.07 mag at J and lower for the other bands (see Table 2 and Fig. 2), therefore we did not apply any additional corrections to the VVV data. This is because the VISTA and 2MASS photometric systems are different, even if the filter names are the same. The VISTA magnitude of an object is not expected to be exactly the same as the 2MASS magnitude (except for an unreddened A0V star) and vice versa.

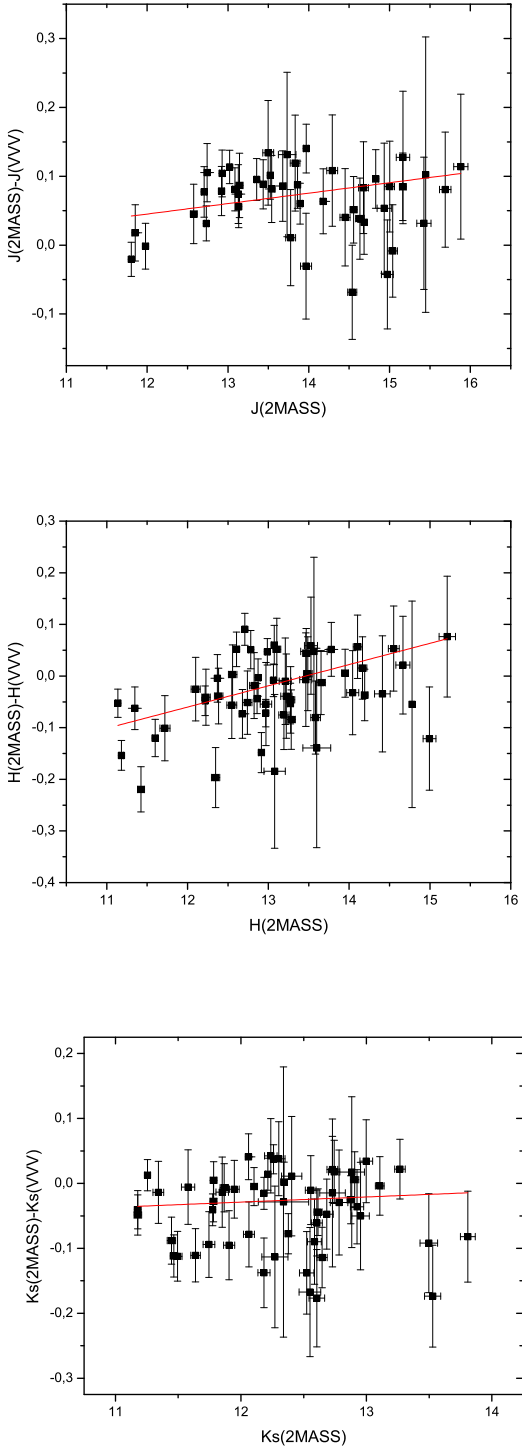
Examining VVV images showed that the detected NIR emission of the PNe, in general, is point-like or nearly so. The larger aperture of the 2MASS photometry will therefore have little effect on the flux of the object, but it can lead to increased contamination by neighbouring stars, especially in crowded fields (very frequent for the bulge region).

#### 4.3. The analysis of the VVV photometry

##### 4.3.1. The ( $J-H$ ) vs. ( $H-K_s$ ) diagram

All known PNe with photometric data in the VVV are placed in the  $J-H$  vs.  $H-K_s$  diagram (Fig. 3). More than 50% are objects with original NIR data. The magnitudes of the sources are listed in Table 3. The magnitudes are not dereddened; the reddening vector, obtained from Saito & et al. (2012) is indicated by the arrow (its length corresponds to 10 mag extinction in V).

PNe belonging to the bulge and disc are plotted separately in the upper panel. The lower panel distinguishes point-like from extended objects, as classified by the pipeline. The interpreta-

**Table 2.** VVV and 2MASS magnitude comparison (linear fit).**Fig. 2.** Comparison between 2MASS and VVV PNe magnitudes.

tion of these diagrams was already discussed in Corradi et al. (2008), and our results are consistent (Ramos-Larios & Phillips 2005, Garcia-Lario et al. 1997, Phillips & Zepeda-García 2009). The expected colours for unreddened main sequence and giant branch stars are shown in the lower diagram, extending from Vega at (0, 0) (in the vicinity of the Rayleigh-Jeans point) to  $(H - K_s, J - H) = (0.5, 1.0)$ . S-type symbiotic stars (and other emission line stars) are located around  $(0.5, 1.0)$ , and for D-type sym-

biotics and T Tau stars a hot dust continuum is added to those to give a broad sequence towards  $(2, 2)$ . Fig. 3 shows that the majority of the VVV PNe are located well away from this, and relatively few are found among the stellar locus.

Compared to the sample of Corradi et al. (2008), there is little evidence for significant further reddening. This is not unexpected as the PNe in our sample had previously been discovered in optical surveys.

To investigate if some difference between PNe populations from disc and bulge is present, we distinguished them in the upper panel of Fig. 3. There is an indication for a separation, with the bulge PNe (black dots) slightly bluer both in  $J - H$  and  $H - K_s$  for objects around the point  $(H - K_s, J - H) = (0.7, 0.5)$  where many of the PNe are found. The separation is much less evident among the objects with stellar colours (presumed field stars). This suggests that the separation is not due to systematic differences in extinction.

As mentioned in Section 2, the VVV pipeline distinguish between stars (point sources) and 'galaxies' (i.e. not point sources). The PNe, according to the flag point-like/not-point-like derived from the VVV pipeline, are plotted in the lower panel of Fig. 3. In general, the analysed sources are interpreted by the pipeline as resolved (66% of the sample shown in Fig. 3). This could be an interesting aid to find new PNe. The distribution of sources within the  $J - H$  vs.  $H - K_s$  plane (Fig. 3, lower panel) shows two concentrations of sources, but the distinction between the stellar and nebular sources only marginally reflects the unresolved/resolved flag. The relation between this flag and the nature of the emission is not obvious.

Interestingly, the stellar locus is sparsely populated compared to other works (for instance Phillips & Zepeda-García 2009). This fact perhaps shows that VVV, with better resolution, yields improved rejection of unrelated field stars. It is noteworthy that there is a distinct concentration near the locus of unreddened K2 stars. This may indicate these are indeed field stars.

The lower panel of Fig. 3 also shows the loci of free-free/bound-free emission from ionised hydrogen gas. These are calculated for a temperature range from 8400 to 17000 K, at approximately  $(H - K_s, J - H) = (0.7, 0.4)$ . The actual measurements deviate from this by about 0.5 mag, especially in  $H - K_s$ . This is mainly due to contributions from emission lines. Interestingly, the bulge PNe tend to be located closer to the bf/ff locus, perhaps reflecting a different emission-line contribution.

We finally compare the observed distribution of PNe with the model of NGC 6720. This gives colours of  $(H - K_s, J - H) = (0.62, 0.0)$ , towards the bottom range of the observed colours. For a similar model for NGC 7027 (Beintema et al. 1996; Zijlstra et al. 2008) we derive unreddened colours of  $(H - K_s, J - H) = (0.21, 0.41)$  also within the general PNe region but close to the blue edge of the PNe distribution. Allowing for a range of extinction values in the observed sample, these two models can cover much of the observed range.

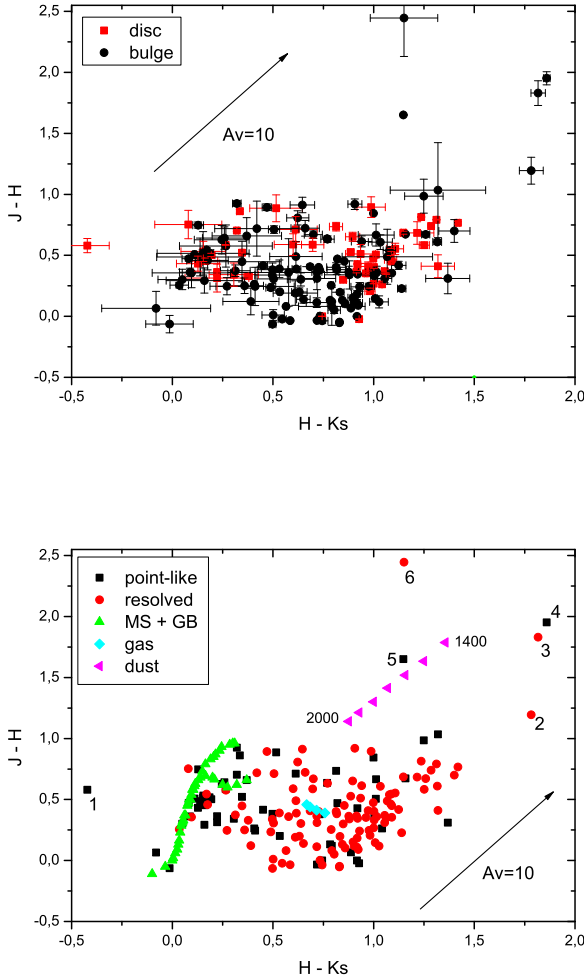


**Fig. 3.** The upper panel shows the distribution of PNe according to whether they belong to the plane or bulge. The lower panel shows the distribution of colour indices ( $H - K_s$ ) and ( $J - H$ ) for the PNe analysed as ‘galaxy-like’ (resolved) by the pipeline, plotted as red circles, point-like sources, plotted as black squares; error bars have been left out for the sake of clarity. The magenta triangles indicate dust emission loci for an emissivity exponent  $\gamma=0$  and temperature  $T_d \leq 2000$  K (in steps of 100 K, Phillips & Cuesta 1994). Intrinsic stellar indices for MS spectral types (Bessell & Brett 1988) and the O-type from Martins et al. (2005) are shown by green triangles. Finally, the free-free and free-bound emission from hydrogen ions are shown for the range of 8400 to 17000 K, by the cyan diamond symbols.

#### 4.3.2. The ( $Y - J$ ) vs. ( $Z - Y$ ) diagram

Figure 4 shows the distribution of PNe in the newly measured ( $Y - J$ ) vs. ( $Z - Y$ ) diagram. We analysed the reddened and dereddened colours (upper and lower panel respectively). In addition, the colours of other emission objects are shown, to be compared with those of PNe. The reddening vector, obtained from Saito & et al. (2012), is indicated by an arrow (its length corresponds to 10 mag extinction in V).

We have extracted from the VVV database the  $Z$ ,  $Y$  and  $J$  magnitudes of symbiotic stars (Belczyński et al. 2000), cataclysmic variables (Downes et al. 2001), Be stars (Zhang et al.

2005), and Mira variables (Kharchenko et al. 2002). Although the samples of these objects are not very large, they are useful to estimate the possible overlap with PNe. The distribution of reddened PNe (Fig. 4, upper panel) occupies a wide region in the ( $Y - J$ ) vs. ( $Z - Y$ ) diagram, but it is possible to isolate an area to the right of the main sequence (MS) and parallel to the reddening vector (limited by the dashed line), which is not shared by the other objects. Although only 41% of PNe are placed to the right of the dashed line, the lack of confusion in this region suggests that this diagram, combined with the standard  $JHK_s$ , will be a useful tool for the identification of new PNe.

The  $ZYJ$  diagnostic diagram, using dereddened colours, is shown in Figure 4 (bottom panel), together with the location of MS stars. The colours are corrected for the interstellar reddening using, in general, the extinction coefficient  $c$  of Tylenda et al. (1992), and by assuming that  $c/E_{B-V} = 1.46$  (Pottasch 1984) and taking the standard  $A/E_{B-V} = 3.1$ . The infrared extinction  $A_Z = 0.499A_V$ ,  $A_Y = 0.390A_V$  and  $A_J = 0.280A_V$  were taken from Saito & et al. (2012). We estimate an uncertainty of 10% on the extinction coefficients  $c$  (see Fig. 4).

There is some overlap in colours between MS stars and unreddened PNe, and this overlap is increased by reddening (top panel). This diagram does not allow us to differentiate PN from MS stars with high efficiency. However, it is evident that the PNe tend to be grouped in a bounded region, and there is a well-defined region containing about half the PNe which is not affected by confusion with the depicted types of objects.

The  $Y$  and  $Z$  bands have strong contributions from emission lines and have less continuum as the bands are relatively narrow (as compared to  $JHK_s$ ). The  $J$ -band contains a strong  $\text{Pa}\beta$  line but also more continuum, as the band is wider. The  $Z - Y$  colour can become negative because the  $Z$ -band contains a strong  $[\text{SIII}]$  line.

#### 4.3.3. Notes on individual objects

A number of objects show unexpected colours. These are labelled by number in Fig. 3, lower panel. The label number is indicated below, after the name of the PN (see Fig. 5).

PN G347.4 + 01.8.— (1) This shows a very blue ( $H - K_s$ ) colour. The  $\text{H}\alpha$  image shows a bipolar morphology (Parker et al. 2006), we identify a VVV NIR source at the geometric centre of the belt, however this could be a spurious star.

PN G001.9 + 02.3.— (2) The colour is indicative of a highly reddened PN. However, we could not reject a very young PN (Ramos-Larios et al. 2009; Lewis 2006).

PN G355.2 – 02.0.— (3) Similar to the previous object, the colour indicates high reddening. The object has a high excitation class (Parker et al. 2006). However, in agreement with Viironen et al. (2009b, Fig. 1) this could be a D-type symbiotic star.

PN G355.0 – 03.3.— (4) Suspected to be a symbiotic star (Miszalski et al. 2009).

PN G356.9 – 05.8.— (5) Its colours can be explained as dominated by hot dust. It is suspected to be a symbiotic star (Miszalski et al. 2009).

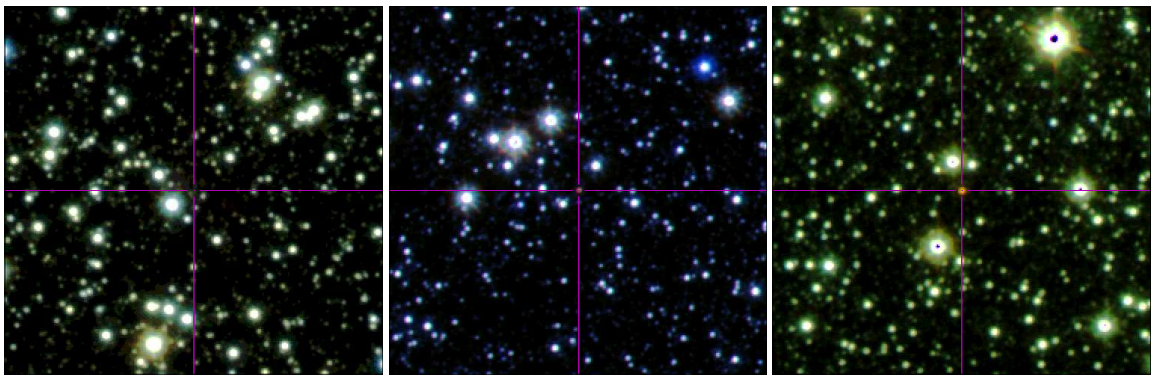


**Fig. 5.**  $JHK_s$  colour composite images showing the six stars (red cross) described at section 4.3.3, range from top left to bottom right. The size of images are  $1.4'$ .

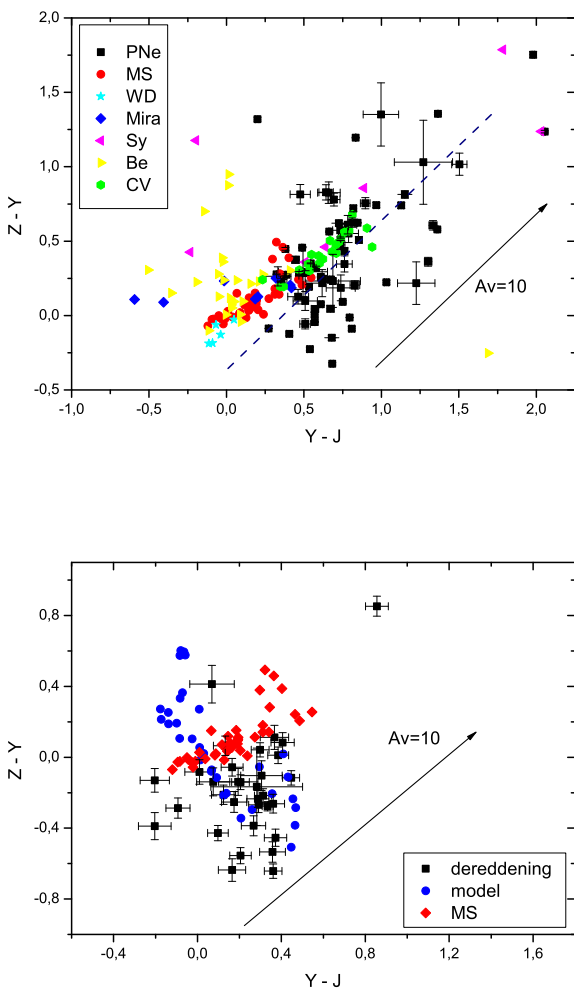


**Fig. 4.** Distribution of the colour indices ( $Y - J$ ) and ( $Z - Y$ ). The upper panel show all detected PNe without applying any extinction correction. Other symbols show other emission-line stars, main sequence stars (Hewett et al. 2006) and white dwarfs (taken from the standard database of MKO) as indicated. The bottom panel shows dereddened colours for the PNe, using the reddening measured from the hydrogen lines. The distribution of the colour indices ( $Y - J$ ) and ( $Z - Y$ ) for a model grid of planetary nebulae is shown in blue.

PN G000.1 – 01.0.— (6) This object has unusual colours. It is a poorly studied object, and perhaps it is not a PN.

#### 4.4. Model distribution

We can again compare the colours of the NGC 6720 model with the observed distribution. The synthetic colour of  $(Y - J, Z - Y) = (0.12, 0.21)$ . The NGC 7027 model has very similar (unreddened) colours of  $(Y - J, Z - Y) = (0.10, 0.24)$ . These fall at the edge of the observed distribution (upper panel of Fig. 4). NGC 7027 is a young, high density PN, whilst NGC 6720 is evolved and has low density. It is therefore not immediately obvious what causes any differences with the observed distribution.

To explore this further, we computed a Cloudy model grid, and for each model in the grid calculated the  $Y - J$  and  $Z - Y$  colours. The grid is defined by varying the effective temperature of the star and the hydrogen density of the nebula. The grid runs from  $\log T_{\text{eff}} = 4.7$  to  $5.4$  in steps of 0.1 dex (temperatures from 50 kK to 250 kK), and from  $\log n_{\text{H}} = 2$  to  $5$  in steps of 1 dex. The model nebula has exactly  $N_{\text{H}} = 10^{57}$  atoms corresponding to a mass of approximately  $1.2 M_{\odot}$ , and all models are calculated up to the outer radius with inclusion of molecular hydrogen in a PDR (Photon Dominated Regions) region, if present.

The lower panel of Fig. 4 shows the distribution of points in the  $(Y - J)$  and  $(Z - Y)$  plane. The models follow the lower edge of the observed PN distribution in the upper panel of Fig. 4. Together with a range of extinction in the VVV sample, the observed distribution can be well explained. There is some discrepancy in the lower panel, in that some dereddened data fall below the model grid. This may reflect limitations in the model grid, such as a constant nebular mass and constant abundances (especially for sulphur). It is also possible that in some cases the extinction coefficient  $c$  of Tytla et al. (1992) is over-estimated, or that the scaling from  $\text{H}\alpha/\text{H}\beta$  to optical and near-infrared broad-band colours is also affected by the shape of the reddening law. Ruffle et al. (2004) have shown indications that the common assumption of  $R = 3.1$  used here may not always be appropriate.

The model grid extends to a region above the stellar locus in the  $(Y - J, Z - Y)$  diagram. There are almost no observed PNe in this region where many of the models fall. These models are those with hottest ionizing stars. At all densities, the  $Z - Y$  colour increases with increasing stellar temperature, as shown in Fig. 6. The largest change occurs between temperatures of  $10^5$  and  $1.25 \times 10^5$  K. The  $Y - J$  curve is largely the mirror image of the  $Z - Y$  curve. This indicates that the change is caused by a high excitation line in the Y band. The  $\text{He I } 1.083\mu\text{m}$  lines decreases

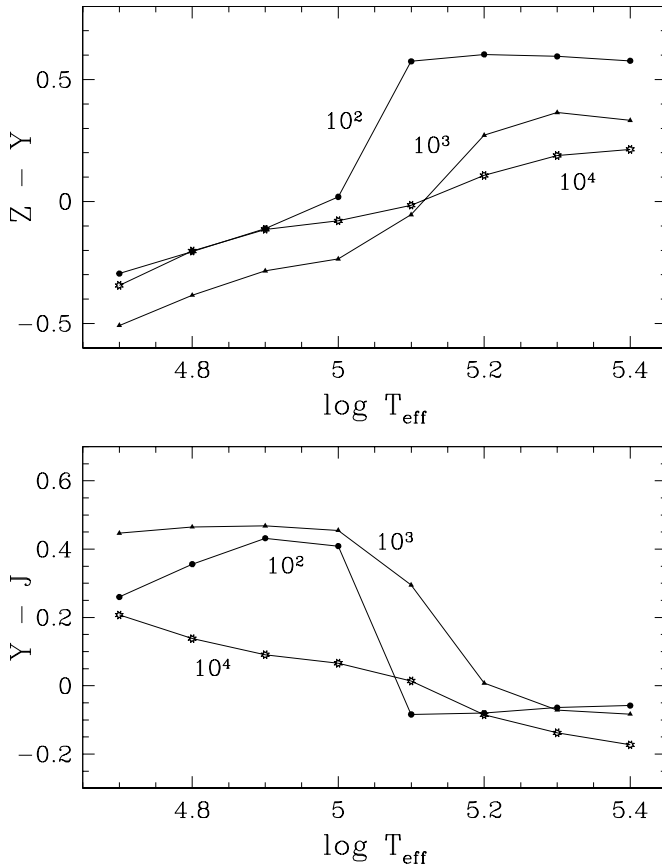


**Fig. 6.** Distribution of the colour indices ( $Y - J$ ) and ( $Z - Y$ ) as function of stellar temperature, for the Cloudy model grid described in the paper. Each curve is for a fixed density, indicated by the adjacent label.

between  $T_{\text{eff}} = 10^5$  en  $10^{5.2}$  K, and the He II  $1.012\mu\text{m}$  becomes much stronger. Both lines are in the Y band, but the latter dominates because of the much higher transmission efficiency at its wavelength (Table 1). The effect is strongest for the lower density models as these are density bounded, and lack any lower ionisation regions. Note that the model in Table 1 is ionisation bounded.

The four model points at  $(Y - J, Z - Y) = (-0.08, 0.55)$  are low density models with  $n_{\text{H}} = 10^2 \text{ cm}^{-3}$ . These are fully ionised and have very large predicted diameters (22 arcsec) at the distance of the bulge. The three models just below this have  $n_{\text{H}} = 10^3, \text{cm}^{-3}$ , are also fully ionised with predicted diameters of 10 arcsec. The nebulae which are missing from the observed distribution are those with very hot stars and large to very large nebulae. Such nebulae may have been removed from the sample (as described above), may not have been included in the VVV catalogues, or their colours have been affected by the use of an aperture much smaller than the size of the nebula.

## 5. Conclusions

The VVV survey is shown to be sensitive to planetary nebulae. Of the 579 known PNe (excluding 75 highly extended objects) in the covered region, 353 have been detected in at least one filter. The majority of these (209) are new near-infrared detections. The NIR images, to the naked eye, suggest compact, point-like sources; however the VVV pipeline classifies a high percentage

of PNe as extended sources. Aperture photometry was obtained from the pipeline catalogues. In the J, H,  $K_s$  bands, the photometry agrees well with 2MASS data where available, in most cases within 0.1 mag, even though 2MASS and VISTA are each on their own photometric system.

We use a photo-ionisation model of NGC 6720 (the Ring nebula) to calculate the flux contributions from emission lines and from the continuum, for each of the five filters. The line contribution decreases with increasing wavelength, from 55% in Z and Y, to 22% in  $K_s$ . The precise contribution depends on the excitation of the nebula, especially at Z and Y where the dominant lines are from sulphur and helium, respectively. The J, H,  $K_s$  bands are dominated by hydrogen, where it should be noted that molecular hydrogen can also contribute at  $K_s$ . Electron temperature and elemental abundances may also affect the relative contributions.

We explore two diagnostic diagrams:  $H - K_s$  vs  $J - H$ , and  $Y - J$  vs  $Z - Y$ . In the former, the PNe are well separated from the stellar locus and from emission line stars. The PNe are located around the colours of the continuum from ionised hydrogen plasmas. Bulge PNe tend to be located closer to these colours than do PNe of the Galactic disc. The reason for this is not clear, but metallicity may play a role. The  $Y - J$  vs  $Z - Y$  diagram shows a broad spread in colours, and PNe have more overlap with the stellar locus. About half fall in a region of the diagram where there is little confusion, so that this diagram can still be a useful tool in finding and classifying PNe.

A model grid was calculated using the Cloudy photo-ionisation code, covering a wide range of stellar temperatures and electron densities, and assuming standard PN abundances. The model spectra were convolved with the VISTA response functions to predict colours. The models show a range of  $Y - J$   $Z - Y$  colours with a sequence approximately perpendicular to the stellar locus. The sequence follows the lower boundary of the distribution of observed PNe; the observed distribution can be reproduced by reddening the model nebulae. There are no observed PNe in the region above the stellar locus, where a significant fraction of the model nebulae are located. These are related to nebulae with hot central stars ( $T > 10^5$  K), where the He II line at  $1.012\mu\text{m}$  becomes the dominant line in Y-band. The missing objects correspond to very large, fully ionised nebula with hot stars which are absent from our selected sample.

The reddening coefficients for many of the observed PNe have been published by Tylenda et al. (1992). When we use these to de-redden our sample, the resulting distribution shows that some objects fit the models very well, but a fraction have colours which are bluer than shown by any of the models. The discrepancy is up to 0.4 mag in  $Y - Z$  and  $J - Y$ . This suggests that the extinction in some nebulae may have been over-estimated. Alternatively, as suggested by Ruffle et al. (2004), uncertainties in the  $R_V$ -value (assumed to be 3.1) may have an effect.

The VVV survey is shown to be a powerful tool to study planetary nebulae in the crowded and extincted region of the galactic plane. The large majority of known objects were detected, but in these regions, many PNe are expected to have remained undiscovered. The results presented here will help locating this missing population in the VVV database.

**Acknowledgements.** We thank the anonymous referee whose very useful remarks helped us to substantially improve this paper. We acknowledge Jim Emerson for comments that helped to improve the paper. This research has made use of the Aladin and SIMBAD database, operated at CDS, Strasbourg, France. This publication makes use of data products from the Two Micron All Sky Survey, a joint Project of the University of Massachusetts and IPAC/CALTECH, funded by NASA and NSF. We gratefully acknowledge use of data from the ESO Public Survey programme ID 179.B-2002 taken with the VISTA telescope, data

products from the Cambridge Astronomical Survey Unit (CASU), and from the VISTA Science Archive at the Wide Field Astronomy Unit (WFAU). PvH acknowledges support from the Belgian Science Policy Office through the ESA PRODEX program. DM gratefully acknowledges funding from the FONDAP Center for Astrophysics 15010003, the BASAL CATA Center for Astrophysics and Associated Technologies PFB-06, the MILENIO Milky Way Millennium Nucleus from the Ministry of Economy's ICM grant P07-021-F, and Proyecto FONDECYT Regular No. 1090213 from CONICYT and the astro-Engineering center at the Universidad Católica (AIUC).

## References

- Acker, A., Marcout, J., Ochsenbein, F., et al. 1992, The Strasbourg-ESO Catalogue of Galactic Planetary Nebulae. Parts I, II (ESO, Garching), ed. Acker, A., Marcout, J., Ochsenbein, F., Stenholm, B., Tylenda, R., & Schohn, C.
- Allen, D. A. 1973, MNRAS, 161, 145
- Beaulieu, S. F., Dopita, M. A., & Freeman, K. C. 1999, ApJ, 515, 610
- Beintema, D. A., van Hoof, P. A. M., Lahuis, F., et al. 1996, A&A, 315, L253
- Belczyński, K., Mikolajewska, J., Munari, U., Ivison, R. J., & Friedjung, M. 2000, A&AS, 146, 407
- Bessell, M. S. & Brett, J. M. 1988, PASP, 100, 1134
- Corradi, R. L. M., Rodríguez-Flores, E. R., Mampaso, A., et al. 2008, A&A, 480, 409
- Cross, N. J. G., Collins, R. S., Mann, R. G., et al. 2012, A&A, 548, A119
- Dalton, G. B., Caldwell, M., Ward, A. K., et al. 2006, in Society of Photo-Optical Instrumentation Engineers (SPIE) Conference Series, Vol. 6269, Society of Photo-Optical Instrumentation Engineers (SPIE) Conference Series
- Downes, R. A., Webbink, R. F., Shara, M. M., et al. 2001, PASP, 113, 764
- Drew, J. E., Greimel, R., Irwin, M. J., et al. 2005, MNRAS, 362, 753
- Emerson, J., McPherson, A., & Sutherland, W. 2006, The Messenger, 126, 41
- Emerson, J. & Sutherland, W. 2010, The Messenger, 139, 2
- Eptein, N., de Batz, B., Capoani, L., et al. 1997, The Messenger, 87, 27
- Ferland, G. J., Korista, K. T., Verner, D. A., et al. 1998, PASP, 110, 761
- Garcia-Lario, P., Manchado, A., Pych, W., & Pottasch, S. R. 1997, A&AS, 126, 479
- Gonzalez, O. A., Rejkuba, M., Zoccali, M., Valenti, E., & Minniti, D. 2011, A&A, 534, A3
- Hewett, P. C., Warren, S. J., Leggett, S. K., & Hodgkin, S. T. 2006, MNRAS, 367, 454
- Hyung, S., Aller, L. H., Feibelman, W. A., & Lee, S.-J. 2001, ApJ, 563, 889
- Irwin, M. J., Lewis, J., Hodgkin, S., et al. 2004, in Society of Photo-Optical Instrumentation Engineers (SPIE) Conference Series, Vol. 5493, Society of Photo-Optical Instrumentation Engineers (SPIE) Conference Series, ed. P. J. Quinn & A. Bridger, 411–422
- Jacoby, G. H. & Van de Steene, G. 2004, A&A, 419, 563
- Kerber, F., Mignani, R. P., Guglielmetti, F., & Wicenc, A. 2003, A&A, 408, 1029
- Kharchenko, N., Kilpio, E., Malkov, O., & Schilbach, E. 2002, A&A, 384, 925
- Kinman, T. D., Feast, M. W., & Lasker, B. M. 1988, AJ, 95, 804
- Lewis, B. M. 2006, in IAU Symposium, Vol. 234, Planetary Nebulae in our Galaxy and Beyond, ed. M. J. Barlow & R. H. Méndez, 449–450
- Maciel, W. J. & Costa, R. D. D. 2003, in IAU Symposium, Vol. 209, Planetary Nebulae: Their Evolution and Role in the Universe, ed. S. Kwok, M. Dopita, & R. Sutherland, 551
- Martins, F., Schaerer, D., & Hillier, D. J. 2005, A&A, 436, 1049
- Minniti, D., Lucas, P. W., Emerson, J. P., et al. 2010, New A, 15, 433
- Miszalski, B., Acker, A., Moffat, A. F. J., Parker, Q. A., & Udalski, A. 2009, A&A, 496, 813
- Miszalski, B., Napiwotzki, R., Cioni, M.-R. L., et al. 2011, A&A, 531, A157
- Miszalski, B., Parker, Q. A., Acker, A., et al. 2008, MNRAS, 384, 525
- Parker, Q. A., Acker, A., Frew, D. J., et al. 2006, MNRAS, 373, 79
- Parker, Q. A., Phillips, S., Pierce, M. J., et al. 2005, MNRAS, 362, 689
- Pena, M. & Torres-Peimbert, S. 1987, Rev. Mexicana Astron. Astrofis., 14, 534
- Petrosian, V. 1976, ApJ, 209, L1
- Phillips, J. P. & Cuesta, L. 1994, A&AS, 104, 169
- Phillips, J. P. & Zepeda-García, D. 2009, MNRAS, 394, 1875
- Pottasch, S. R., ed. 1984, Astrophysics and Space Science Library, Vol. 107, Planetary nebulae - A study of late stages of stellar evolution
- Ramos-Larios, G., Guerrero, M. A., Suárez, O., Miranda, L. F., & Gómez, J. F. 2009, A&A, 501, 1207
- Ramos-Larios, G. & Phillips, J. P. 2005, MNRAS, 357, 732
- Rauch, T. 2003, A&A, 403, 709
- Rudy, R. J., Lynch, D. K., Mazuk, S., Puetter, R. C., & Dearborn, D. S. P. 2001, AJ, 121, 362
- Ruffle, P. M. E., Zijlstra, A. A., Walsh, J. R., et al. 2004, MNRAS, 353, 796
- Saito, R. K. & et al. 2012, A&A, 537, A107
- Skrutskie, M. F., Cutri, R. M., Stiening, R., et al. 2006, AJ, 131, 1163
- Tylenda, R., Acker, A., Stenholm, B., & Koeppen, J. 1992, A&AS, 95, 337
- van Hoof, P. A. M. 2000, MNRAS, 314, 99
- van Hoof, P. A. M., van de Steene, G. C., Barlow, M. J., et al. 2010, A&A, 518, L137
- Viironen, K., Greimel, R., Corradi, R. L. M., et al. 2009a, A&A, 504, 291
- Viironen, K., Mampaso, A., Corradi, R. L. M., et al. 2009b, A&A, 502, 113
- Whitelock, P. A. 1985, MNRAS, 213, 59
- Yasuda, N., Fukugita, M., Narayanan, V. K., et al. 2001, AJ, 122, 1104
- Zhang, P., Chen, P. S., & Yang, H. T. 2005, New A, 10, 325
- Zijlstra, A. A., van Hoof, P. A. M., & Perley, R. A. 2008, ApJ, 681, 1296

**Table 3.** NIR photometry catalogue of PNe (aperture 1.41''). The marks “:” and “\*” refer to near saturation and probable not central star of PN, respectively. While the mark “†” refer to the new NIR determination.

name	PN G	$\alpha$ (2000)	$\delta$ (2000)	OT	Z	$\sigma Z$	Y	$\sigma Y$	J	$\sigma J$	H	$\sigma H$	$K_s$	$\sigma K_s$
JaSt 71 †	000.0-01.2	17 50 23.21	-28 33 10.65	-1	-	-	-	-	-	-	-	-	12.888	0.026
H 1-62	000.0-06.8	18 13 17.96	-32 19 42.92	1	-	-	-	-	13.005	0.002	13.041	0.004	12.456	0.004
JaSt 69 †	000.1-01.0	17 50 10.01	-29 19 04.28	1	-	-	-	-	17.833	0.221	15.387	0.095	14.236	0.072
M 3-43	000.1-01.1	17 50 24.34	-29 25 18.46	1	-	-	-	-	13.684	0.005	12.96	0.011	-	-
JaSt 75	000.1-01.2	17 50 47.99	-29 24 43.43	1	-	-	-	-	14.407	0.01	13.738	0.021	13.038	0.024
H 2-40 †	000.1-05.6	18 08 30.76	-31 36 35.12	1	-	-	-	-	15.764	0.035	15.305	0.043	15.13	0.06
Ae 2-J †	000.1+02.6	17 35 35.45	-27 24 05.31	-1	15.607	0.017	15.044	0.018	-	-	-	-	-	-
H 1-16	000.1+04.3	17 29 23.39	-26 26 05.11	1	-	-	-	-	13.055	0.003	12.603	0.004	11.749	0.003
JaSt 79	000.2-01.4	17 51 53.55	-29 30 53.56	-1	14.886	0.016	13.133	0.005	11.153:	0.002	10.309:	0.002	9.31:	0.001
SB 1 †	000.2-01.9	17 53 45.64	-29 43 46.92	1	15.571	0.029	14.743	0.023	14.1	0.024	-	-	-	-
M 2-19 †	000.2-04.6	18 04 44.15	-31 02 48.62	1	-	-	-	-	-	-	-	-	14.003	0.028
MPA1800-3023 †	000.3-03.4	18 00 11.1	-30 23 49.39	1	-	-	17.592	0.32	-	-	-	-	-	-
PPA1730-2621 †	000.3+04.2	17 30 12.35	-26 21 01.10	-1	-	-	-	-	15.592	0.02	15.21	0.035	14.712	0.041
M 2-28	000.4-01.9	17 54 25.32	-29 36 08.18	1	12.978	0.004	12.682	0.005	-	-	-	-	10.659:	0.003
JaSt 36 †	000.4+01.1	17 42 25.12	-27 55 36.35	1	-	-	-	-	14.568	0.023	13.959	0.037	12.926	0.023
PPA1729-2611	000.4+04.4	17 29 52.37	-26 11 13.47	1	-	-	-	-	15.039	0.012	14.797	0.024	13.867	0.019
M 3-19 †	000.5-01.6	17 53 25.06	-29 17 07.91	1	-	-	-	-	-	-	-	-	14.099	0.088
K 6-7 †	000.5+01.9	17 39 31.21	-27 27 45.87	1	-	-	16.163	0.052	15.442	0.051	14.951	0.072	14.337	0.059
JaSt 74 †	000.7-00.8	17 50 46.83	-28 44 35.11	1	-	-	-	-	-	-	-	-	12.916	0.027
M 2-21	000.7-02.7	17 58 09.59	-29 44 20.01	1	14.457	0.013	13.824	0.01	-	-	13.262	0.017	12.282	0.009
M 3-22 †	000.7-03.7	18 02 19.23	-30 14 26.01	1	-	-	-	-	-	-	-	-	15.301	0.131
He 2-250 †	000.7+03.2	17 34 54.75	-26 35 57.22	1	-	-	15.596	0.017	15.11	0.019	14.807	0.035	14.169	0.032
H 2-46	000.8-07.6	18 18 37.46	-31 54 45.31	1	16.06	0.014	16.115	0.021	15.608	0.013	15.496	0.026	14.778	0.027
JaSt 78 †	000.9-00.9	17 51 24.62	-28 35 40	-1	-	-	-	-	-	-	-	-	12.283	0.015
MPA1751-2838 †	000.9-01.0	17 51 43.26	-28 38 58.62	-1	-	-	-	-	-	-	-	-	13.314	0.037
Bl 3-13 †	000.9-02.0	17 56 02.78	-29 11 16.64	1	15.415	0.034	15.311	0.05	-	-	-	-	13.69	0.046
PPA1740-2708 †	000.9+01.8	17 40 51.79	-27 08 48.94	1	18.508	0.236	-	-	17.231	0.26	-	-	15.234	0.135
Sa 3-104	001.0-02.6	17 58 25.91	-29 20 48.54	-1	15.376	0.034	15.372	0.054	-	-	-	-	12.07	0.011
Sa 3-92 †	001.1-01.6	17 54 52.09	-28 48 54.99	1	16.24	0.074	-	-	-	-	-	-	13.839	0.053
SB 4 †	001.1-06.4	18 14 14.14	-31 11 09.70	-1	17.778	0.08	17.484	0.087	16.99	0.071	16.503	0.085	16.365	0.13
JaSt 54 †	001.1+00.8	17 45 11.12	-27 32 38.06	1	-	-	-	-	14.69	0.026	13.968	0.038	13.307	0.033
MPA1739-2648 †	001.1+02.2	17 39 49.71	-26 48 45.48	-1	-	-	16.7	0.082	15.841	0.074	14.856	0.065	13.607	0.03
JaSt 95 †	001.2-01.2a	17 53 35.29	-28 28 51.02	-1	-	-	-	-	-	-	-	-	13.057	0.024
SAWI 5	001.2-03.9	18 03 53.68	-29 51 22.14	-1	-	-	-	-	-	-	-	-	11.874	0.004
JaSt 56 *	001.2+00.7	17 45 46.88	-27 30 41.94	1	-	-	-	-	14.334	0.014	12.77	0.011	12.045	0.011
He 2-262	001.2+02.1	17 40 12.86	-26 44 21.94	1	-	-	14.665	0.014	14.544	0.022	13.624	0.021	12.717	0.013
SB 5 †	001.3-05.6	18 11 15.42	-30 37 50	-1	-	-	-	-	15.285	0.025	15.348	0.046	15.362	0.072
PPA1800-2904 †	001.5-02.8	18 00 22.42	-29 04 39.23	1	17.279	0.237	16.877	0.224	-	-	-	-	-	-
SwSt 1	001.5-06.7	18 16 12.27	-30 52 07.98	-1	10.935:	0.001	11.021:	0.001	10.749:	0.001	10.748:	0.001	9.831:	0.001
JaSt 46 †	001.5+01.5	17 43 30.37	-26 47 32.63	1	-	-	-	-	14.184	0.017	13.824	0.034	12.808	0.021
K 5-5	001.5+03.6	17 35 22.12	-25 42 47	1	-	-	15.432	0.014	14.606	0.012	14.296	0.022	13.241	0.014
JaSt 63 †	001.6+00.1	17 48 46.2	-27 25 36.78	1	-	-	-	-	-	-	15.808	0.091	-	-
H 1-55	001.7-04.4	18 07 14.57	-29 41 24.58	1	-	-	-	-	-	-	-	-	13.039	0.012

**Table 3.** continued.

name	PN G	$\alpha$ (2000)	$\delta$ (2000)	OT	Z	$\sigma Z$	Y	$\sigma Y$	J	$\sigma J$	H	$\sigma H$	$K_s$	$\sigma K_s$
H 1-56	001.7-04.6	18 07 53.89	-29 44 34.41	1	-	-	-	-	-	-	-	-	13.439	0.017
JaSt 52	001.7+01.3	17 44 37.23	-26 47 25.4	-1	-	-	-	-	-	-	-	-	12.001	0.008
PHR1735-2527 †	001.7+03.6	17 35 47.31	-25 27 42.32	1	-	-	-	-	17.875	0.2	-	-	15.939	0.203
JaSt 81	001.8-00.5	17 52 04.28	-27 36 38	1	-	-	-	-	-	-	-	-	12.529	0.012
PHR1804-2913 †	001.8-03.7	18 04 28.51	-29 13 57.15	-2	14.74	0.019	14.463	0.02	-	-	-	-	13.219	0.014
SAWI 7 †	001.8-03.8	18 05 05.54	-29 20 15.75	1	-	-	-	-	-	-	-	-	12.984	0.011
MPA1742-2613 †	001.9+01.9	17 42 45.81	-26 13 47.22	-1	16.453	0.034	16.031	0.043	15.308	0.042	14.667	0.051	14.408	0.058
K 5-10	001.9+02.3	17 41 24.52	-26 03 53.36	1	-	-	16.652	0.075	15.759	0.064	14.565	0.046	12.782	0.013
M 2-33	002.0-06.2	18 15 06.57	-30 15 33.26	1	-	-	-	-	13.805	0.004	13.869	0.008	13.371	0.009
MPA1747-2649 †	002.0+00.7	17 47 28.35	-26 49 48.82	-1	-	-	-	-	-	-	-	-	13.626	0.037
MPA1755-2741 †	002.1-01.1	17 55 10.4	-27 41 39.78	-1	-	-	-	-	-	-	-	-	12.921	0.017
M 3-20	002.1-02.2	17 59 19.33	-28 13 48.4	1	-	-	-	-	-	-	-	-	12.613	0.016
H 1-54	002.1-04.2	18 07 07.28	-29 13 06.14	1	-	-	-	-	-	-	-	-	11.864	0.004
JaFu 1 †	002.1+01.7	17 43 57.24	-26 11 53.7	1	-	-	-	-	-	-	-	-	14.064	0.041
M 2-23	002.2-02.7	18 01 42.64	-28 25 44.1	-1	12.776	0.003	12.594	0.004	-	-	12.125	0.006	11.356	0.005
H 1-63	002.2-06.3	18 16 19.34	-30 07 36.15	-1	-	-	-	-	12.907	0.002	12.941	0.004	12.223	0.003
Ta 2337 *	002.2+00.5	17 48 45.15	-26 43 27.03	-1	-	-	-	-	16.276	0.027	14.573	0.025	13.841	0.033
H 2-37 †	002.3-03.4	18 04 28.83	-28 37 38.32	1	15.953	0.057	16.143	0.093	-	-	15.566	0.132	14.978	0.136
M 2-41 *	002.3-07.8	18 22 34.49	-30 43 29.12	-1	17.707	0.055	17.044	0.04	17.598	0.082	17.45	0.16	-	-
PPA1803-2826 †	002.4-03.1	18 03 24.72	-28 26 26.1	1	15.862	0.051	15.883	0.073	-	-	15.737	0.156	-	-
M 1-38 †	002.4-03.7	18 06 05.74	-28 40 29.85	1	-	-	12.911	0.005	-	-	12.502	0.008	12.424	0.013
KnFs 14 †	002.5-05.4	18 13 00.88	-29 25 11.5	-1	-	-	-	-	15.631	0.034	15.329	0.05	15.279	0.071
M 1-37	002.6-03.4	18 05 25.8	-28 22 04.42	1	13.334	0.005	13.196	0.006	-	-	12.619	0.009	12.019	0.009
Th 3-27 †	002.6+04.2	17 35 58.5	-24 25 29.37	1	-	-	-	-	14.257	0.007	14.029	0.013	12.89	0.008
H 2-20	002.8+01.7	17 45 39.81	-25 40 00.39	1	-	-	-	-	-	-	-	-	12.451	0.012
Ta 1567 †	002.8+01.8	17 45 28.31	-25 38 11.78	1	-	-	-	-	16.984	0.19	16.453	0.308	-	-
H 2-39 †	002.9-03.9	18 08 05.77	-28 26 10.74	1	-	-	-	-	-	-	-	-	13.646	0.02
KnFs 12 †	003.2-04.4	18 10 30.83	-28 19 22.95	-1	-	-	-	-	-	-	-	-	16.082	0.173
M 2-36	003.2-06.2	18 17 41.42	-29 08 19.74	1	-	-	-	-	13.369	0.003	13.367	0.005	12.634	0.005
KnFs 19 †	003.3-07.5	18 23 08.93	-29 43 25.86	1	-	-	-	-	17.413	0.071	17.283	0.129	17.31	0.276
IC 4673 †	003.5-02.4	18 03 18.44	-27 06 22.71	1	-	-	15.95	0.039	-	-	-	-	-	-
M 2-14	003.6+03.1	17 41 57.27	-24 11 16.2	1	13.348	0.003	13.672	0.006	12.989	0.004	12.842	0.007	11.834	0.004
K 5-6 †	003.6+04.9	17 35 31.25	-23 11 48.79	1	-	-	-	-	-	-	-	-	15.147	0.065
M 2-30 †	003.7-04.6	18 12 34.41	-27 58 10.36	1	-	-	-	-	-	-	-	-	13.209	0.013
PHR1802-2637 †	003.8-01.9	18 02 11.27	-26 37 08.09	-1	-	-	15.265	0.022	-	-	-	-	-	-
PHR1804-2653 †	003.8-02.4	18 04 02.59	-26 53 25.84	1	17.632	0.097	16.997	0.109	-	-	-	-	-	-
H 1-59 †	003.8-04.3	18 11 29.22	-27 46 14.72	1	-	-	-	-	-	-	-	-	12.606	0.007
H 2-41 †	003.8-04.5	18 12 23.67	-27 52 13.85	1	-	-	-	-	-	-	-	-	16.293	0.214
KnFs 11 †	004.1-03.8	18 10 12.24	-27 16 34.97	1	-	-	-	-	-	-	-	-	15.159	0.075
PPA1741-2332 †	004.1+03.6	17 41 28.81	-23 32 19.07	-1	19.078	0.435	18.557	0.422	17.375	0.223	16.34	0.166	15.021	0.071
H 1-60	004.2-04.3	18 12 25.22	-27 29 12.74	1	-	-	-	-	-	-	-	-	12.666	0.008
M 2-37 †	004.2-05.9	18 18 38.35	-28 07 58.51	-1	-	-	-	-	16.591	0.052	16.281	0.073	14.913	0.037
PPA1801-2553 †	004.3-01.4	18 01 18.9	-25 53 21.21	1	-	-	15.544	0.028	-	-	-	-	13.204	0.018
H 2-24 †	004.3+01.8	17 48 36.55	-24 16 33.95	-1	13.924	0.004	12.568	0.002	11.203:	0.001	10.567:	0.001	9.798:	0.001

**Table 3.** continued.

name	PN G	$\alpha$ (2000)	$\delta$ (2000)	OT	Z	$\sigma Z$	Y	$\sigma Y$	J	$\sigma J$	H	$\sigma H$	$K_s$	$\sigma K_s$
SB 9 †	004.6–09.9	18 35 42.15	-29 38 24.77	1	-	-	19.521	0.253	-	-	-	-	-	-
PHR1801-2522 †	004.8–01.1	18 01 16.91	-25 22 39.33	1	-	-	-	-	-	-	-	-	12.836	0.011
M 3-26 †	004.8–05.0	18 16 11.44	-27 14 57.82	1	-	-	-	-	16.939	0.094	-	-	-	-
H 2-25	004.8+02.0	17 49 00.51	-23 42 54.82	1	14.354	0.006	14.161	0.008	13.629	0.008	13.395	0.013	12.906	0.012
H 2-42 †	005.0–03.9	18 12 22.98	-26 32 54.14	1	-	-	-	-	-	-	-	-	14.067	0.026
Pe 1-9 †	005.0+03.0	17 45 36.78	-23 02 26.18	-1	17.367	0.08	17.134	0.099	16.448	0.08	15.931	0.098	15.779	0.13
H 1-58	005.1–03.0	18 09 13.84	-26 02 28.94	-1	-	-	13.548	0.005	-	-	-	-	-	-
Hf 2-2 †	005.1–08.9	18 32 30.91	-28 43 20.37	-1	-	-	-	-	17.468	0.058	17.824	0.197	-	-
K 5-19 †	005.1+02.0	17 49 51.43	-23 27 45.45	1	17.018	0.069	-	-	-	-	16.109	0.157	-	-
PPA1803-2516	005.2–01.6	18 03 52.38	-25 16 59.31	-1	14.437	0.004	13.488	0.003	-	-	-	-	-	-
IRAS18023-2513 †	005.4–01.9	18 05 25.38	-25 13 35.76	1	17.205	0.044	16.506	0.048	-	-	-	-	-	-
SB 12 †	005.4–06.1	18 21 55.21	-27 09 46.78	1	-	-	-	-	16.569	0.05	16.213	0.073	16.118	0.122
H 1-34 †	005.5+02.7	17 48 07.67	-22 46 47.49	-1	14.4	0.007	14.549	0.012	13.869	0.01	13.502	0.014	12.499	0.008
KnFs 16 †	005.6–04.7	18 16 53.91	-26 23 22.09	-1	-	-	-	-	16.492	0.062	16.246	0.096	15.835	0.098
KnFs 13 †	005.7–03.6	18 12 44.67	-25 44 20.16	1	18.422	0.219	-	-	-	-	-	-	-	-
M 2-38 †	005.7–05.3	18 19 25.13	-26 35 19.46	1	-	-	-	-	-	-	16.88	0.172	-	-
M 2-31	006.0–03.6	18 13 16.04	-25 30 05.45	1	-	-	14.029	0.008	-	-	-	-	-	-
Th 4-3	006.0+02.8	17 48 37.42	-22 16 49.35	-1	14.474	0.007	14.188	0.009	13.677	0.009	13.262	0.012	12.811	0.011
M 1-28 †	006.0+03.1	17 47 38.31	-22 06 20.22	1	-	-	-	-	17.754	0.268	-	-	-	-
PPA1756-2311 †	006.1+00.8	17 56 33.16	-23 11 47.14	1	17.387	0.036	-	-	-	-	-	-	-	-
MPA1751-2223	006.3+02.2	17 51 40.01	-22 23 18.3	1	-	-	-	-	-	-	-	-	13.448	0.017
M 1-31	006.4+02.0	17 52 41.45	-22 21 57.16	1	-	-	-	-	-	-	-	-	11.607	0.003
H 1-61	006.5–03.1	18 12 33.98	-24 50 00.49	1	14.102	0.004	14.011	0.005	13.26	0.004	12.905	0.006	11.815	0.004
H 2-45 †	006.8–03.4	18 14 28.75	-24 43 38	1	15.344	0.01	15.097	0.013	14.474	0.013	14.275	0.021	13.644	0.018
Ae 1	006.8–08.6	18 34 55.25	-27 06 19.21	1	-	-	-	-	16.263	0.019	15.649	0.027	14.709	0.025
Pe 2-10	006.8+02.0	17 53 37.21	-21 58 42	-1	-	-	-	-	-	-	-	-	11.274	0.003
MPA1755-2212 †	006.9+01.5	17 55 36.69	-22 12 47.91	1	17.597	0.043	16.919	0.044	-	-	-	-	-	-
H 1-66 †	007.0–06.0	18 24 57.32	-25 41 54.63	1	-	-	-	-	-	-	16.19	0.058	-	-
Vy 2-1	007.0–06.8	18 27 59.62	-26 06 48.09	1	-	-	-	-	13.014	0.002	13.061	0.004	12.23	0.003
SB 14 †	007.7–05.3	18 23 42.54	-24 47 28.05	-1	-	-	-	-	16.528	0.05	16.664	0.116	17.607	0.471
M 2-34 †	007.8–03.7	18 17 16.02	-23 58 54.8	1	15.831	0.016	15.751	0.023	-	-	-	-	-	-
M 2-39	008.1–04.7	18 22 01.15	-24 10 39.93	-1	-	-	-	-	12.987	0.002	12.314	0.003	11.156	0.002
M 2-42	008.2–04.8	18 22 32.07	-24 09 27.61	1	-	-	-	-	14.409	0.008	14.446	0.015	13.702	0.013
NGC 6644	008.3–07.3	18 32 34.7	-25 07 44.15	1	-	-	-	-	11.852	0.001	11.719	0.001	10.875:	0.001
H 1-64 †	008.4–03.6	18 18 23.83	-23 24 57.39	1	16.381	0.026	16.283	0.038	15.775	0.04	15.654	0.069	15.263	0.071
PPA1813-2233 †	008.6–02.2	18 13 10.61	-22 33 26.66	1	17.249	0.038	16.396	0.035	15.341	0.027	-	-	14.487	0.039
MaC 1-11	008.6–02.6	18 14 50.89	-22 43 55.7	1	15.311	0.01	14.877	0.011	14.115	0.009	13.727	0.012	13.111	0.01
Th 4-5 †	009.0+04.1	17 50 28.36	-19 03 09.27	1	17.277	0.039	-	-	-	-	-	-	-	-
Th 4-9	009.3+02.8	17 56 00.60	-19 29 26.74	-1	15.481	0.007	14.867	0.007	-	-	-	-	12.2	0.005
Th 4-6	009.3+04.1	17 50 57.24	-18 46 48.4	1	15.538	0.009	15.359	0.011	-	-	-	-	-	-
SB 16 †	009.4–05.6	18 28 21.32	-23 25 25.02	1	17.117	0.032	16.867	0.035	-	-	-	-	-	-
PPA1831-2356 †	009.4–06.6	18 31 56.36	-23 56 07.79	-1	-	-	-	-	16.855	0.038	16.561	0.066	16.402	0.124
MPA1815-2113 †	010.0–02.0	18 15 36.98	-21 13 21.44	1	-	-	-	-	15.168	0.018	14.804	0.028	13.927	0.021
MPA1157-6226 †	296.7–00.2	11 57 47.62	-62 26 22.09	1	19.695	0.142	18.343	0.07	17.346	0.045	16.451	0.04	15.464	0.03

**Table 3.** continued.

name	PN G	$\alpha$ (2000)	$\delta$ (2000)	OT	Z	$\sigma Z$	Y	$\sigma Y$	J	$\sigma J$	H	$\sigma H$	$K_s$	$\sigma K_s$
PHR1202-6112 †	297.0+01.1	12 02 17.93	-61 12 47.73	1	-	-	-	-	-	-	-	-	16.9	0.092
PHR1213-6344 †	298.7-01.1	12 13 46.39	-63 45 00.66	-1	15.602	0.004	15.09	0.004	14.353	0.003	13.649	0.003	13.328	0.004
MPA1221-6413	299.7-01.5	12 21 51.92	-64 13 05.70	1	16.599	0.008	15.278	0.005	15.079	0.006	14.393	0.006	13.246	0.004
PHR1223-6236 *	299.7+00.1	12 23 57.88	-62 36 18.16	-1	-	-	-	-	17.723	0.056	16.533	0.038	16.016	0.048
He 2-84 †	300.4-00.9	12 28 46.84	-63 44 37.26	1	15.893	0.004	15.446	0.005	15.066	0.006	14.765	0.008	13.916	0.008
MPA1235-6318 †	301.1-00.4	12 35 21.47	-63 18 00.69	1	-	-	-	-	17.308	0.042	16.624	0.05	15.408	0.033
PN 1231-6401	301.1-01.4	12 34 35.99	-64 18 16.79	1	-	-	14.882	0.004	14.917	0.006	14.15	0.005	12.731	0.003
MPA1242-6459	301.9-02.1	12 42 24.21	-64 59 24.77	1	-	-	15.204	0.005	14.504	0.004	14.138	0.005	13.223	0.004
MPA1243-6428	302.0-01.6	12 43 19.42	-64 28 01.34	1	-	-	-	-	14.684	0.005	13.944	0.004	12.658	0.003
MPA1249-6414 †	302.6-01.3	12 49 14.52	-64 14 27.36	1	-	-	-	-	17.149	0.041	16.738	0.052	15.419	0.031
PHR1250-6346 †	302.7-00.9	12 50 04.46	-63 46 52.54	1	-	-	-	-	18.988	0.206	18.294	0.239	18.126	0.409
PHR1257-6052 †	303.6+01.9	12 57 09.50	-60 52 36.19	-2	-	-	20.124	0.281	19.015	0.162	18.491	0.198	17.93	0.269
MPA1309-6415 †	304.8-01.4	13 09 31.08	-64 15 32.8	1	-	-	-	-	15.108	0.007	14.778	0.009	14.402	0.012
He 2-90 †	305.1+01.4	13 09 36.23	-61 19 35.98	-1	-	-	-	-	11.263:	0.001	-	-	9.622:	0.001
PHR1318-6358 †	305.9-01.2	13 18 50.76	-63 58 54.26	-1	-	-	-	-	13.638	0.002	12.58	0.002	-	-
MPA1319-6418 †	305.9-01.6	13 19 24.06	-64 18 53.44	1	-	-	-	-	15.981	0.016	15.573	0.021	14.601	0.015
PHR1324-6418 †	306.4-01.6	13 24 11.88	-64 18 10.38	-1	-	-	-	-	16.872	0.04	16.34	0.044	16.186	0.066
PHR1324-6448 †	306.4-02.1	13 24 32.18	-64 48 12.04	-1	-	-	-	-	13.024	0.002	12.502	0.002	12.156	0.002
MPA1326-6407 †	306.7-01.5	13 26 32.61	-64 07 10.3	-2	-	-	-	-	15.332	0.01	-	-	14.085	0.01
PHR1327-6032 †	307.3+02.0	13 27 13.5	-60 32 11.74	1	-	-	-	-	17.658	0.057	16.906	0.059	16.827	0.107
MPA1327-6031 †	307.3+02.0a	13 27 30.47	-60 31 58.61	-1	-	-	-	-	16.409	0.058	15.696	0.047	15.083	0.06
PHR1341-6427 †	308.2-02.1	13 41 07.41	-64 27 53.58	1	-	-	-	-	-	-	15.935	0.028	14.224	0.011
PHR1335-6015 †	308.3+02.1	13 35 02.69	-60 15 43.35	-1	-	-	-	-	13.462	0.002	12.877	0.002	12.612	0.003
WeKG 2 †	308.4+00.4	13 38 42.55	-61 55 45.77	-1	-	-	-	-	14.593	0.004	14.11	0.005	13.85	0.008
MPA1346-6418 †	308.8-02.0	13 46 41.43	-64 18 46.31	1	-	-	18.052	0.055	-	-	17.192	0.088	16.482	0.083
He 2-96	309.0+00.8	13 42 36.16	-61 22 28.89	-1	-	-	-	-	12.532	0.001	12.269	0.001	11.227	0.001
MPA1354-6337	309.8-01.6	13 54 22.39	-63 37 17.97	1	-	-	-	-	15.015	0.006	14.644	0.009	13.589	0.006
WeKG 3 †	310.6+01.4	13 54 24.63	-60 27 22.27	-1	-	-	-	-	15.898	0.011	15.444	0.014	15.283	0.05
PHR1408-6229 †	311.7-00.9	14 08 47.25	-62 29 59.6	1	18.949	0.056	18.577	0.067	-	-	-	-	16.401	0.14
He 2-106	312.0-02.0	14 14 09.41	-63 25 46.24	-1	12.052:	0.001	10.521:	0	-	-	-	-	-	-
PN 1412-5947	313.3+01.1	14 15 53.28	-60 01 37.83	1	15.767	0.004	15.188	0.004	13.828	0.002	13.013	0.002	11.777	0.001
BeVa 1	313.7+02.1	14 16 51.85	-58 53 10	1	-	-	-	-	13.773	0.002	13.425	0.003	12.363	0.002
MPA1428-6234	313.8-01.7	14 28 50.87	-62 34 13.53	-1	17.583	0.022	16.804	0.021	16.11	0.018	15.375	0.018	14.561	0.015
PHR1420-5933 †	313.9+01.4	14 20 06.76	-59 33 53.7	-2	-	-	-	-	17.407	0.045	-	-	15.746	0.042
MPA1430-6251 †	314.0-02.1	14 30 52.66	-62 51 14.67	1	17.889	0.029	17.278	0.033	16.496	0.025	15.909	0.029	15.211	0.027
PHR1438-6140 †	315.2-01.3	14 38 18.16	-61 40 01.03	1	-	-	-	-	18.538	0.192	-	-	17.04	0.161
MPA1441-6114	315.7-01.1	14 41 32.18	-61 14 17.95	1	-	-	-	-	14.594	0.006	14.048	0.006	12.961	0.004
PN 1434-5858	316.2+00.8	14 38 20	-59 11 46.13	-2	-	-	14.416	0.003	13.348	0.002	12.555	0.001	11.243	0.001
PHR1447-6127 †	316.3-01.6	14 47 37.84	-61 27 22.23	-1	-	-	-	-	-	-	-	-	-	-
MPA1439-5816 †	316.7+01.6	14 39 25.05	-58 16 01.66	1	17.524	0.025	17.177	0.03	16.416	0.021	15.863	0.025	14.756	0.017
PHR1453-5714 †	318.8+01.8	14 53 24.94	-57 14 49.49	-1	18.481	0.047	17.888	0.055	-	-	-	-	16.077	0.095
PHR1507-5925 †	319.5-01.0	15 07 50.22	-59 25 15.01	1	17.489	0.015	17.045	0.019	-	-	-	-	15.467	0.064
He 2-117	320.9+02.0	15 05 59.22	-55 59 16.56	1	12.694	0.001	12.707	0.001	11.911	0.001	11.643	0.001	10.643:	0.001
MPA1522-5917 †	321.2-01.9	15 22 58.24	-59 17 44.41	1	16.828	0.012	16.622	0.016	15.794	0.015	15.329	0.019	14.245	0.012

**Table 3.** continued.

name	PN G	$\alpha$ (2000)	$\delta$ (2000)	OT	Z	$\sigma Z$	Y	$\sigma Y$	J	$\sigma J$	H	$\sigma H$	$K_s$	$\sigma K_s$
BMP1522-5729	322.2-00.4	15 22 58.98	-57 29 59.54	1	15.744	0.004	15.247	0.005	-	-	-	-	12.988	0.007
BMP1524-5746 †	322.2-00.7	15 24 24.08	-57 46 21.4	1	16.144	0.005	15.384	0.005	-	-	-	-	12.389	0.004
Pe 2-8	322.4-00.1	15 23 42.9	-57 09 25.24	-1	-	-	12.836	0.001	11.826	0.001	11.848	0.001	10.92:	0.001
MPA1523-5710 †	322.4-00.1a	15 23 22.59	-57 10 48.21	1	-	-	-	-	-	-	15.863	0.032	14.425	0.018
MPA1517-5538 *	322.5+01.5	15 17 24.52	-55 38 22.53	-1	-	-	-	-	19.103	0.226	17.915	0.174	17.406	0.195
MPA1530-5801	322.7-01.4	15 30 50.95	-58 01 28.67	1	16.59	0.009	15.847	0.008	14.88	0.006	14.353	0.008	13.466	0.006
MPA1520-5517 †	323.1+01.6	15 20 29.75	-55 17 43.02	1	-	-	-	-	-	-	-	-	16.185	0.196
PHR1539-5727 †	324.0-01.6	15 39 34.8	-57 27 02.20	-1	14.605	0.002	14.149	0.002	13.661	0.003	13.298	0.004	13.075	0.005
He 2-133	324.8-01.1	15 41 58.82	-56 36 25.74	1	13.74	0.001	13.116	0.001	12.27	0.001	11.821	0.001	10.731:	0.001
PHR1551-5653 †	325.6-02.1	15 51 20.59	-56 53 50.68	-1	17.39	0.027	17.126	0.038	16.795	0.047	16.481	0.068	16.259	0.09
VB 2 †	325.9-01.7	15 51 18.83	-56 21 21.8	-1	16.41	0.012	15.691	0.011	14.872	0.008	14.01	0.007	13.675	0.008
VB 3 †	326.1-01.9	15 52 59.04	-56 24 26.1	1	18.369	0.066	-	-	-	-	17.369	0.157	16.838	0.15
He 2-140	327.1-01.8	15 58 08.09	-55 41 50.4	1	13.332	0.001	13.343	0.002	-	-	12.424	0.002	11.578	0.001
He 2-142	327.1-02.2	15 59 57.61	-55 55 33.1	-1	12.736	0.001	12.477:	0.001	11.868	0.001	11.439	0.001	10.519:	0.001
He 2-143 †	327.8-01.6	16 00 59.14	-55 05 40.05	1	13.529	0.001	13.178	0.001	12.634	0.001	12.16	0.001	11.162	0.001
PN 1557-5445	328.0-01.6	16 01 50.86	-54 53 40.01	-1	15.499	0.006	15.276	0.008	14.244	0.005	13.737	0.006	12.726	0.004
Lo 10 †	328.2+01.3	15 49 28.96	-52 30 16.12	-2	-	-	-	-	-	-	-	-	14.516	0.024
PHR1552-5254 †	328.3+00.7	15 52 56.8	-52 54 11.28	1	-	-	-	-	-	-	-	-	16.816	0.23
MPA1606-5407 †	329.1-01.4	16 06 38.77	-54 07 20.8	1	-	-	15.182	0.007	14.276	0.005	13.873	0.007	12.871	0.004
MPA1605-5319	329.5-00.8	16 05 37.41	-53 19 54.19	1	17.355	0.015	16.749	0.017	15.416	0.01	14.833	0.015	13.581	0.01
VBRC 7 †	329.5+01.7	15 54 50.61	-51 22 34.78	1	-	-	-	-	-	-	18.174	0.233	-	-
PHR1557-5128 *	329.7+01.4	15 57 07.38	-51 27 59.28	-2	19.063	0.062	18.475	0.075	17.705	0.074	15.946	0.034	14.252	0.014
He 2-153 †	330.6-02.1	16 17 14.23	-53 32 07.50	1	-	-	-	-	-	-	-	-	16.841	0.182
PN 1600-5041	331.0+01.2	16 04 17.88	-50 50 02.55	-1	15.487	0.004	15.2	0.005	14.732	0.006	14.229	0.008	14.035	0.011
MPA1618-5147 †	332.0-01.0	16 18 42.73	-51 47 44.57	1	-	-	-	-	-	-	14.743	0.015	14.143	0.018
BMP1622-5144 †	332.4-01.4	16 22 34.05	-51 44 55.8	-1	17.477	0.033	17.291	0.053	16.553	0.04	16.212	0.056	15.907	0.067
PHR1619-4907 †	334.0+00.7	16 19 49.89	-49 06 54.56	-1	-	-	-	-	-	-	18.803	0.474	17.663	0.384
PHR1633-4650 †	337.3+00.6	16 33 57.93	-46 50 07.02	-1	-	-	17.895	0.061	16.77	0.049	15.884	0.061	15.369	0.07
Pe 1-7	337.4+01.6	16 30 25.85	-46 02 50.88	-1	12.569	0.001	12.302:	0.001	11.834	0.001	11.834	0.001	11.089	0.001
PHR1634-4628 †	337.6+00.7	16 34 51.27	-46 28 28.37	-1	16.469	0.009	16.227	0.013	15.871	0.022	15.439	0.04	15.311	0.067
MPA1650-4747	338.4-02.0	16 50 09.81	-47 47 04.84	1	18.288	0.042	17.272	0.032	15.768	0.017	15.115	0.02	14.219	0.015
MPA1635-4458	338.8+01.7	16 35 10.37	-44 58 40.59	1	16.411	0.01	15.902	0.011	15.047	0.009	14.841	0.015	13.859	0.01
PHR1639-4516 †	339.1+00.9	16 39 22.45	-45 16 35.54	-2	-	-	18.587	0.123	-	-	-	-	16.712	0.26
MPA1703-4450 †	342.1-02.0	17 03 23.98	-44 50 30.37	1	17.033	0.017	16.323	0.017	-	-	-	-	14.278	0.024
PN 1652-4341	342.2-00.3	16 56 33.95	-43 46 14.74	1	-	-	14.63	0.003	-	-	-	-	11.406	0.002
Vd 1-9	343.0-01.7	17 05 38.93	-43 56 20.14	1	-	-	-	-	-	-	-	-	12.9	0.008
PHR1707-4309 †	343.9-01.6	17 07 57.16	-43 09 05.74	-1	-	-	-	-	-	-	-	-	14.337	0.029
PN 1708-4227	344.9-01.9	17 12 22.05	-42 30 41.51	1	-	-	-	-	-	-	-	-	12.199	0.004
MPA1713-4015	346.8-00.7	17 13 10.83	-40 15 56.22	1	-	-	-	-	-	-	-	-	12.9	0.009
PHR1709-3931 *	347.0+00.3	17 09 10.31	-39 31 04.88	-1	18.08	0.025	17.246	0.022	16.265	0.017	15.287	0.021	15.342	0.046
PHR1714-4006 †	347.2-00.8	17 14 49.42	-40 06 08.14	1	-	-	-	-	-	-	-	-	15.452	0.091
PPA1704-3824 †	347.4+01.6	17 04 59.13	-38 24 04.41	1	17.742	0.028	17.191	0.032	16.403	0.033	15.891	0.045	14.956	0.03
PHR1704-3819 †	347.4+01.8	17 04 16.84	-38 19 57.68	-1	17.434	0.021	16.862	0.023	16.127	0.026	15.548	0.032	15.97	0.076
Vd 1-8	347.7+02.0	17 04 33.79	-37 53 15.28	1	14.651	0.002	14.087	0.002	13.424	0.003	13.071	0.003	12.11	0.002

**Table 3.** continued.

name	PN G	$\alpha$ (2000)	$\delta$ (2000)	OT	Z	$\sigma Z$	Y	$\sigma Y$	J	$\sigma J$	H	$\sigma H$	$K_s$	$\sigma K_s$
MPA1717-3945 †	347.8-01.1	17 17 49.33	-39 45 58.69	1	-	-	-	-	-	-	-	-	13.203	0.009
PPA1705-3748 †	347.9+01.9	17 05 27.11	-37 48 48.45	1	18.101	0.039	17.275	0.034	16.614	0.039	16.025	0.05	15.425	0.045
H 1-22	350.8-02.4	17 32 22.15	-37 57 23.85	1	-	-	-	-	13.783	0.004	13.665	0.009	12.761	0.006
MPA1737-3837 †	350.8-03.6	17 37 05.28	-38 37 17.09	1	-	-	-	-	15.873	0.025	15.535	0.043	15.038	0.044
H 2-1	350.9+04.4	17 04 36.25	-33 59 18.82	-1	-	-	-	-	11.455:	0.001	11.335	0.001	10.542:	0.001
PHR1712-3452 †	351.1+02.6	17 12 19.04	-34 52 07.23	-1	16.488	0.016	16.302	0.022	-	-	-	-	-	-
M 1-19	351.1+04.8	17 03 46.84	-33 29 44.41	1	-	-	-	-	13.216	0.002	13.269	0.004	12.439	0.004
PPA1738-3753 †	351.5-03.4	17 38 11.01	-37 53 40.72	1	-	-	-	-	16.38	0.043	16.04	0.072	15.16	0.052
MPA1736-3717 †	351.8-02.7	17 36 10.12	-37 17 08.09	1	-	-	-	-	17.906	0.173	-	-	16.441	0.167
Sa 2-215	351.9-01.9	17 33 00.66	-36 43 51.81	1	-	-	-	-	11.982	0.001	11.58	0.002	10.853:	0.002
H 1-30	352.0-04.6	17 45 06.80	-38 08 49.76	1	-	-	-	-	14.651	0.008	14.499	0.014	13.601	0.011
PPA1737-3650 †	352.4-02.7	17 37 37.65	-36 50 18.17	1	-	-	-	-	15.732	0.024	15.425	0.04	14.922	0.042
SB 37 †	352.6-04.9	17 47 52.7	-37 48 02.54	1	-	-	-	-	16.041	0.024	15.79	0.04	15.431	0.055
H 1-8	352.6+03.0	17 14 42.93	-33 24 47.43	1	14.593	0.005	14.456	0.006	-	-	-	-	-	-
SB 38	352.7-08.4	18 03 29.04	-39 21 26.79	-1	13.301	0.002	13.024	0.002	12.7	0.001	12.265	0.002	-	-
PPA1715-3313 †	352.8+03.0	17 15 10.4	-33 13 47.58	1	-	-	17.324	0.075	-	-	-	-	-	-
PPA1718-3315 †	353.2+02.4	17 18 44.96	-33 15 24.9	1	17.548	0.033	16.732	0.029	-	-	-	-	-	-
SB 39	353.3-08.3	18 04 31.68	-38 47 39.35	-1	14.494	0.003	14.22	0.003	13.834	0.003	13.325	0.003	13.215	0.006
K 5-8	353.4-02.4	17 39 17.15	-35 46 59.41	-1	14.604	0.005	13.368	0.003	11.314:	0.001	10.843:	0.001	10.024:	0.001
PPA1722-3317	353.6+01.7	17 22 35.38	-33 17 14.49	1	16.384	0.013	16.023	0.016	14.721	0.008	14.111	0.014	12.795	0.008
MPA1719-3247 †	353.6+02.6	17 19 10.16	-32 47 23.16	1	-	-	17.994	0.091	-	-	-	-	-	-
MPA1711-3112 †	354.0+04.8	17 11 37.06	-31 12 21.57	1	-	-	-	-	-	-	-	-	15.347	0.061
M 2-10 †	354.2+04.3	17 14 07.02	-31 19 43.02	1	-	-	-	-	-	-	-	-	13.513	0.011
Th 3-4	354.5+03.3	17 18 51.94	-31 39 06.60	1	14.818	0.005	14.405	0.006	-	-	-	-	-	-
PPA1737-3414 †	354.6-01.4	17 37 53.93	-34 14 27.39	-1	-	-	-	-	15.511	0.037	14.844	0.054	13.832	0.035
PPA1721-3149 †	354.7+02.8	17 21 23.75	-31 49 52.22	1	16.611	0.019	16.408	0.03	-	-	-	-	-	-
PPA1725-3216 †	354.8+01.8	17 25 15.87	-32 16 11.52	1	16.676	0.02	15.752	0.016	-	-	-	-	-	-
MPA1744-3444 †	354.9-02.8	17 44 43.58	-34 44 25.32	1	17.899	0.178	17.311	0.153	16.45	0.113	15.731	0.113	15.311	0.096
Th 3-6	354.9+03.5	17 19 20.24	-31 12 40.87	1	15.663	0.01	15.735	0.017	-	-	-	-	-	-
PPA1746-3454	355.0-03.3	17 46 51.42	-34 54 05.62	-1	16.788	0.064	16.57	0.079	15.346	0.041	13.394	0.013	11.534	0.003
K 5-18 †	355.0-03.7	17 48 29.6	-35 05 28.7	1	-	-	-	-	17.402	0.272	-	-	-	-
PPA1722-3139	355.0+02.6	17 22 40.8	-31 39 55.28	1	15.718	0.009	15.266	0.011	-	-	-	-	-	-
Th 3-11	355.1+02.3	17 24 26.33	-31 43 19.89	1	15.934	0.01	15.466	0.013	-	-	-	-	-	-
Ta 140 †	355.1+04.7	17 15 03.03	-30 20 37.22	-1	-	-	-	-	16.382	0.056	15.754	0.061	15.508	0.075
PPA1741-3405 †	355.2-02.0	17 41 59.08	-34 05 34.46	1	18.218	0.166	17.187	0.116	15.916	0.072	14.086	0.029	12.269	0.007
H 1-29	355.2-02.5	17 44 13.87	-34 17 33.36	1	14.359	0.005	14.039	0.007	13.46	0.008	13.052	0.011	12.368	0.008
Ta 137 †	355.2+03.7	17 19 03.44	-30 53 54.68	1	18.641	0.132	18.42	0.198	-	-	-	-	-	-
M 3-14	355.4-02.4	17 44 20.63	-34 06 40.64	1	14.026	0.004	14.251	0.008	13.712	0.01	13.528	0.017	12.61	0.01
Hf 2-1 †	355.4-04.0	17 51 12.18	-34 55 22.98	1	-	-	-	-	15.163	0.028	14.916	0.042	14.645	0.042
H 1-32 †	355.6-02.7	17 46 06.33	-34 03 45.87	1	13.685	0.004	13.608	0.006	12.999	0.005	12.897	0.008	12.039	0.005
H 1-33 †	355.7-03.0	17 47 49.42	-34 08 05.13	1	14.6	0.009	14.554	0.013	13.883	0.011	13.518	0.015	12.801	0.01
H 2-23	355.7-03.4	17 48 57.91	-34 21 54.39	-1	14.889	0.012	14.515	0.012	14.069	0.013	13.321	0.012	13.193	0.014
H 1-35	355.7-03.5	17 49 13.93	-34 22 52.63	-1	12.006:	0.001	12.049:	0.002	11.478:	0.001	11.411	0.002	10.523:	0.001
MPA1728-3132 †	355.8+01.7	17 28 31.09	-31 32 08.86	1	-	-	-	-	14.704	0.01	14.072	0.017	13.301	0.016

**Table 3.** continued.

name	PN G	$\alpha$ (2000)	$\delta$ (2000)	OT	Z	$\sigma Z$	Y	$\sigma Y$	J	$\sigma J$	H	$\sigma H$	$K_s$	$\sigma K_s$
M 1-30	355.9-04.2	17 52 58.94	-34 38 22.64	1	-	-	-	-	-	-	-	-	12.322	0.006
Th 3-10	355.9+02.7	17 24 40.9	-30 51 59.52	1	-	-	15.056	0.014	-	-	-	-	12.676	0.011
PPA1723-3038 †	355.9+03.1	17 23 23.54	-30 38 40.16	1	-	-	-	-	-	-	-	-	14.506	0.045
H 1-9	355.9+03.6	17 21 31.9	-30 20 48.81	1	12.99	0.002	12.827	0.002	-	-	-	-	11.218	0.002
PPA1743-3315 †	356.0-01.8	17 43 07.17	-33 15 54.05	1	-	-	-	-	15.197	0.03	14.283	0.033	13.638	0.027
PPA1724-3043 †	356.0+02.8	17 24 58.38	-30 43 03.98	-2	-	-	16.503	0.054	-	-	-	-	14.007	0.036
H 2-26 †	356.1-03.3	17 49 50.97	-34 00 32.06	1	16.944	0.064	-	-	-	-	-	-	15.687	0.19
Th 3-13	356.1+02.7	17 25 19.38	-30 40 41.92	-1	-	-	14.444	0.009	-	-	-	-	11.956	0.006
Cn 2-1	356.2-04.4	17 54 33.01	-34 22 21.16	1	-	-	-	-	-	-	-	-	11.74	0.003
PPA1726-3045 †	356.2+02.5	17 26 23.52	-30 45 38.85	1	17.002	0.052	16.231	0.048	15.026	0.028	14.219	0.031	13.596	0.024
MPA1725-3033 †	356.2+02.7	17 25 33.43	-30 33 56.54	1	-	-	17.444	0.121	-	-	-	-	14.873	0.078
MPA1751-3339 †	356.5-03.4	17 51 20.7	-33 39 14	-1	15.437	0.016	14.813	0.015	14.001	0.013	13.076	0.011	12.756	0.011
H 2-27	356.5-03.6	17 51 50.58	-33 47 36.24	1	15.391	0.016	14.916	0.016	14.182	0.015	13.47	0.015	12.965	0.013
H 1-39	356.5-03.9	17 53 21.02	-33 55 58.4	1	-	-	-	-	-	-	-	-	12.708	0.008
Th 3-55 †	356.5+01.5	17 30 58.86	-31 01 05.70	1	-	-	-	-	14.478	0.014	14.094	0.027	13.277	0.021
MPA1757-3410 †	356.7-04.7	17 57 00.54	-34 10 40.86	1	-	-	-	-	17.382	0.158	16.899	0.186	-	-
H 1-41 †	356.7-04.8	17 57 19.11	-34 09 48.88	1	-	-	-	-	14.864	0.016	14.854	0.028	14.353	0.027
K 5-20 †	356.8-03.0	17 50 10.77	-33 14 17.99	1	16.44	0.039	16.222	0.052	15.604	0.054	15.522	0.101	14.73	0.064
H 2-35 †	356.8-05.4	18 00 18.27	-34 27 40.36	1	-	-	-	-	17.553	0.186	-	-	-	-
Th 3-12	356.8+03.3	17 25 06.13	-29 45 16.91	1	14.775	0.007	14.369	0.008	-	-	-	-	12.263	0.006
M 2-24	356.9-05.8	18 02 02.89	-34 27 47.24	-1	-	-	-	-	12.842	0.003	11.191	0.001	10.043:	0.001
PPA1734-3102	356.9+00.9	17 34 34.37	-31 02 07.64	1	-	-	-	-	14.31	0.012	13.892	0.022	12.768	0.013
MPA1729-3016 †	356.9+02.2	17 29 23.21	-30 16 48.13	-1	17.148	0.123	16.613	0.138	15.981	0.066	15.321	0.084	14.951	0.089
M 3-38	356.9+04.4	17 21 04.48	-29 02 59.57	1	-	-	-	-	13.996	0.008	13.664	0.011	12.662	0.006
M 2-11 †	356.9+04.5	17 20 33.26	-29 00 39.01	1	-	-	-	-	13.938	0.007	13.74	0.011	12.906	0.008
H 1-43	357.1-04.7	17 58 14.44	-33 47 37.7	-1	-	-	-	-	13.077	0.003	12.876	0.005	12.342	0.005
M 3-7 †	357.1+03.6	17 24 34.46	-29 24 19.67	1	13.943	0.004	13.883	0.006	-	-	-	-	12.482	0.007
SB 49	357.2-09.8	18 20 09.34	-36 07 21.43	1	-	-	-	-	15.393	0.008	15.138	0.015	15.103	0.031
Ae 2-H †	357.2+01.4	17 33 17.03	-30 26 29.67	1	-	-	-	-	15.996	0.055	-	-	-	-
H 2-13 †	357.2+02.0	17 31 08.11	-30 10 28.16	1	-	-	15.356	0.019	-	-	-	-	13.331	0.019
PPA1747-3215 †	357.3-02.0	17 47 28.52	-32 15 46.2	1	16.324	0.014	15.511	0.012	14.359	0.01	13.82	0.018	12.742	0.012
M 3-41	357.3+03.3	17 25 59.81	-29 21 50.25	1	13.71	0.004	13.524	0.004	-	-	12.544	0.006	12.31	0.007
PHR1752-3244 †	357.4-03.1	17 52 00.28	-32 44 10.1	-1	18.433	0.289	17.873	0.279	17.822	0.495	17.487	0.687	17.043	0.612
M 2-16	357.4-03.2	17 52 34.37	-32 45 51.48	1	13.876	0.005	13.999	0.008	13.593	0.01	13.484	0.017	12.566	0.01
M 2-18	357.4-03.5	17 53 37.85	-32 58 47.81	1	14.176	0.006	14.17	0.01	13.6	0.01	13.548	0.019	12.745	0.012
M 2-22	357.4-04.6	17 58 32.58	-33 28 36.74	1	-	-	-	-	13.764	0.009	13.219	0.01	13.049	0.009
SB 51 †	357.4-07.2	18 09 16.51	-34 47 41.94	-1	-	-	-	-	15.111	0.008	14.638	0.011	14.557	0.022
M 3-42 †	357.5+03.2	17 26 59.82	-29 15 32.06	1	16.417	0.038	-	-	-	-	-	-	-	-
H 2-29 †	357.6-03.3	17 53 16.82	-32 40 38.52	1	-	-	17.804	0.26	-	-	-	-	-	-
H 1-23	357.6+01.7	17 32 46.92	-30 00 14.99	1	14.084	0.005	14.172	0.008	13.364	0.008	13.116	0.016	12.14	0.01
H 1-18	357.6+02.6	17 29 42.76	-29 32 50.25	1	14.087	0.005	14.005	0.007	-	-	-	-	12.196	0.008
PPA1734-3004 †	357.7+01.4	17 34 46.63	-30 04 21.49	1	-	-	-	-	15.962	0.084	15.474	0.142	14.406	0.083
M 1-34 †	357.9-05.1	18 01 22.21	-33 17 43.74	1	-	-	-	-	-	-	15.744	0.07	15.023	0.069
PPA1750-3152 †	358.0-02.4	17 50 48.56	-31 52 27.35	1	-	-	16.77	0.075	-	-	-	-	-	-

**Table 3.** continued.

name	PN G	$\alpha$ (2000)	$\delta$ (2000)	OT	Z	$\sigma Z$	Y	$\sigma Y$	J	$\sigma J$	H	$\sigma H$	$K_s$	$\sigma K_s$
Th 3-23	358.0+02.6	17 30 21.36	-29 10 12.77	1	16.035	0.026	14.813	0.015	-	-	-	-	12.73	0.015
H 2-10	358.2+03.5	17 27 32.87	-28 31 06.81	1	15.267	0.014	-	-	-	-	13.858	0.02	13.003	0.013
M 3-10	358.2+03.6	17 27 20.18	-28 27 51.16	1	13.947	0.004	-	-	-	-	13.024	0.009	12.143	0.006
H 1-17	358.3+03.0	17 29 40.61	-28 40 22.13	-1	13.941	0.004	-	-	-	-	12.752	0.007	11.839	0.005
JaSt 2 †	358.4+01.7	17 35 00.93	-29 22 15.33	1	-	-	17.285	0.142	-	-	-	-	-	-
Th 3-19	358.4+03.3	17 28 41.81	-28 27 19.62	-1	15.497	0.017	-	-	-	-	13.468	0.014	12.774	0.01
JaSt 64 †	358.5-01.7	17 48 56.03	-31 06 42.77	1	15.982	0.01	15.241	0.01	14.114	0.008	13.443	0.013	12.184	0.007
M 4-7 †	358.5-02.5	17 51 44.71	-31 36 00.86	1	15.929	0.01	15.308	0.01	14.582	0.012	14.18	0.026	13.366	0.021
H 1-46	358.5-04.2	17 59 02.51	-32 21 43.47	1	-	-	-	-	12.637	0.003	12.555	0.005	11.99	0.003
Ae 2-F †	358.5+02.9	17 30 30.44	-28 35 55.07	1	17.334	0.207	16.838	0.166	16.276	0.096	-	-	15.416	0.154
M 3-51 †	358.6-05.5	18 04 56.24	-32 54 00.99	1	-	-	-	-	16.659	0.075	16.21	0.091	15.864	0.103
JaSt 16 †	358.6+00.7	17 39 22.68	-29 41 46.11	1	-	-	-	-	15.109	0.04	14.41	0.054	13.009	0.023
M 4-6	358.6+01.8	17 35 13.99	-29 03 10.34	1	15.205	0.013	14.679	0.013	-	-	-	-	12.394	0.011
Ae 2-R	358.7-02.7	17 53 36.47	-31 25 25.87	-1	12.692	0.002	11.496:	0.001	10.661:	0.001	10.283:	0.001	9.55:	0.001
Th 3-15 †	358.8+04.0	17 27 10.64	-27 43 58.17	1	-	-	-	-	15.755	0.027	15.366	0.044	14.834	0.045
SrWe 2 †	358.8+04.1	17 27 00.33	-27 40 34.55	-2	-	-	-	-	16.833	0.073	16.257	0.1	15.991	0.131
M 1-26	358.9-00.7	17 45 57.67	-30 12 00.70	-1	-	-	-	-	10.128:	0	9.995:	0.001	9.212:	0.001
M 2-26 †	358.9-00.7	18 03 11.92	-26 58 31.3	1	-	-	16.28	0.053	-	-	-	-	-	-
JaSt 65 †	358.9-01.5	17 49 19.98	-30 36 06.26	1	15.162	0.02	14.408	0.017	13.512	0.014	12.618	0.013	12.148	0.011
H 1-44 †	358.9-03.7	17 58 10.65	-31 42 56.01	1	-	-	-	-	14.62	0.019	14.502	0.03	13.475	0.016
H 1-20	358.9+03.2	17 30 43.81	-28 04 06.79	1	14.184	0.004	14.361	0.007	-	-	-	-	-	-
H 1-19 †	358.9+03.4	17 30 02.56	-27 59 18.01	1	14.19	0.004	14.813	0.011	-	-	-	-	-	-
M 2-25 †	359.0-04.8	18 02 46.56	-32 09 29.48	1	-	-	-	-	17.63	0.192	-	-	-	-
Ae 2-G †	359.0+02.8	17 32 22.58	-28 14 28.9	-1	15.431	0.014	14.841	0.014	-	-	-	-	-	-
M 3-16 †	359.1-02.3	17 52 46.05	-30 49 35.2	1	15.156	0.02	15.03	0.03	14.567	0.037	14.376	0.063	13.765	0.047
M 3-46 †	359.1-02.9	17 55 05.61	-31 12 16	1	17.133	0.134	16.848	0.152	16.091	0.125	15.731	0.151	15.153	0.151
JaSt 8 †	359.2+01.3	17 38 27.72	-28 51 59.99	-1	-	-	-	-	16.838	0.18	16.093	0.274	15.56	0.273
Th 3-14	359.2+04.7	17 25 44.08	-26 57 47.95	-1	-	-	-	-	13.054	0.003	12.792	0.004	12.384	0.005
Hb 5	359.3-00.9	17 47 56.19	-29 59 39.51	1	-	-	-	-	11.731:	0.001	11.386	0.003	10.465:	0.002
M 3-17	359.3-03.1	17 56 25.65	-31 04 17.38	1	14.273	0.008	14.228	0.012	13.657	0.012	13.516	0.02	12.866	0.014
SB 54 †	359.3-06.0	18 08 31.39	-32 29 54.41	-1	-	-	-	-	15.327	0.015	14.965	0.019	14.877	0.033
Th 3-35	359.3+01.4	17 38 42.22	-28 42 45.86	-2	-	-	-	-	15.22	0.041	-	-	-	-
Ae 2-E †	359.3+03.6	17 30 14.42	-27 30 20.35	1	17.235	0.053	16.505	0.049	-	-	-	-	-	-
PPA1809-3233 †	359.4-06.3	18 09 52.83	-32 33 44.34	-1	-	-	-	-	16.728	0.05	16.662	0.088	16.742	0.182
SB 55	359.4-08.5	18 19 26.59	-33 37 07.04	-1	15.184	0.005	14.943	0.005	14.594	0.005	14.076	0.007	13.891	0.011
PPA1735-2809 †	359.4+02.3a	17 35 12.12	-28 09 31.49	1	17.354	0.078	16.985	0.102	-	-	-	-	-	-
Ae 2-K †	359.5+02.6	17 34 13.86	-27 56 01.99	1	-	-	15.833	0.039	-	-	-	-	-	-
H 2-36 †	359.6-04.8	18 04 07.80	-31 39 11.95	1	-	-	-	-	17.387	0.218	16.984	0.283	-	-
Ae 2-I †	359.6+02.2	17 36 14.2	-28 00 46.27	1	16.276	0.03	15.59	0.028	-	-	-	-	-	-
M 3-45 †	359.7-01.8	17 52 05.97	-30 05 14	1	15.827	0.037	15.012	0.029	14.537	0.036	14.226	0.056	13.508	0.038
H 1-40	359.7-02.6	17 55 36.05	-30 33 32.32	1	13.544	0.004	13.302	0.005	12.628	0.005	12.373	0.007	11.585	0.004
M 2-32 †	359.8-07.2	18 14 50.61	-32 36 55.22	1	-	-	-	-	14.322	0.005	14.344	0.009	13.798	0.012
Th 3-33 †	359.8+02.4	17 35 48.13	-27 43 20.28	1	15.163	0.011	15.249	0.021	-	-	-	-	-	-
Th 3-25 †	359.8+03.7	17 30 46.73	-27 05 59.79	1	14.961	0.007	14.695	0.01	-	-	-	-	-	-

**Table 3.** continued.

name	PN G	$\alpha$ (2000)	$\delta$ (2000)	OT	Z	$\sigma Z$	$Y$	$\sigma Y$	J	$\sigma J$	H	$\sigma H$	$K_s$	$\sigma K_s$
M 2-27	359.9–04.5	18 03 52.6	−31 17 46.8	1	−	−	−	−	12.823	0.004	12.732	0.006	11.808	0.004
SB 56	359.9–07.4	18 15 32.47	−32 38 00.26	1	−	−	−	−	16	0.019	15.626	0.028	15.314	0.045

**Table 4.** Petrosian radius of the 353 PNe listed in Table 3. When  $\sigma=0$  means that  $\sigma < 0.05$  and when  $\sigma \equiv n$  means that there is only one measured so it is not possible to give an stdev.

name	P <sub>Z</sub>	$\sigma$	P <sub>Y</sub>	$\sigma$	P <sub>J</sub>	$\sigma$	P <sub>H</sub>	$\sigma$	P <sub>K<sub>s</sub></sub>	$\sigma$
Ae 1	-	-	-	-	2.2	0.7	1.2	0.1	1.5	0.2
Ae 2-E	3.0	1.2	2.9	0.4	-	-	-	-	-	-
Ae 2-F	2.8	0.8	1.7	0.1	1.7	n	-	-	1.8	n
Ae 2-G	1.7	0.2	1.6	0.0	-	-	-	-	-	-
Ae 2-H	-	-	-	-	2.2	n	1.7	n	1.7	0.1
Ae 2-I	3.2	0.0	3.1	0.1	-	-	-	-	-	-
Ae 2-J	2.9	0.0	2.5	0.0	-	-	-	-	-	-
Ae 2-K	-	-	3.3	0.0	-	-	-	-	-	-
Ae 2-R	1.8	0.2	2.0	0.0	2.0	0.2	2.5	0.3	2.2	0.3
BeVa 1	2.1	0.0	2.1	0.0	1.7	0.0	1.7	0.0	1.9	0.1
Bl 3-13	3.3	0.4	2.6	0.5	2.9	0.3	2.4	n	2.4	0.2
BMP1522-5729	3.3	0.4	3.3	0.4	3.3	0.7	3.6	0.1	3.3	0.3
BMP1524-5746	2.2	0.0	2.1	0.0	2.0	0.0	2.0	0.0	2.1	0.0
BMP1622-5144	1.8	0.1	1.8	0.1	1.5	0.2	1.6	0.3	1.5	0.2
Cn 2-1	-	-	-	-	2.0	0.0	1.9	0.0	1.9	0.1
H 1-8	3.3	0.0	3.1	0.0	-	-	-	-	-	-
H 1-9	2.6	0.5	2.6	0.3	2.8	0.1	2.3	0.0	2.0	0.1
H 1-16	-	-	-	-	2.3	0.0	2.2	0.1	2.2	0.1
H 1-17	2.6	0.3	2.3	0.1	2.6	0.3	1.8	0.1	1.5	0.0
H 1-18	2.3	0.1	2.1	0.0	-	-	-	-	1.9	0.0
H 1-19	1.6	0.0	1.3	0.1	-	-	-	-	-	-
H 1-20	3.0	0.0	2.9	0.0	-	-	-	-	-	-
H 1-22	-	-	-	-	3.0	0.0	3.1	0.2	2.9	0.0
H 1-23	2.4	0.0	2.3	0.0	2.3	0.0	2.2	0.0	2.3	0.0
H 1-29	2.4	0.0	2.4	0.0	2.4	0.1	2.2	0.1	2.1	0.1
H 1-30	-	-	-	-	2.4	0.0	2.0	0.0	2.1	0.1
H 1-32	2.4	0.6	1.7	0.0	1.6	0.1	1.4	0.0	1.4	0.0
H 1-33	2.5	0.2	2.4	0.2	2.2	0.0	2.1	0.1	2.1	0.0
H 1-34	2.0	0.0	1.9	0.0	1.6	0.0	1.6	0.0	1.5	0.1
H 1-35	2.3	0.0	2.1	0.0	1.8	0.1	1.6	0.0	1.6	0.0
H 1-39	-	-	-	-	2.0	0.1	1.7	0.0	1.9	0.1
H 1-40	2.2	0.1	2.1	0.1	1.7	0.0	1.6	0.1	1.6	0.1
H 1-41	-	-	-	-	4.3	0.6	3.6	0.3	4.7	0.8
H 1-43	-	-	-	-	1.6	0.0	1.5	0.1	1.6	0.1
H 1-44	-	-	-	-	2.8	0.1	3.2	0.4	3.2	0.3
H 1-46	-	-	-	-	1.8	0.3	2.0	0.7	1.6	0.2
H 1-54	-	-	-	-	1.5	0.0	1.5	0.1	1.5	0.1
H 1-55	-	-	-	-	2.1	0.0	2.2	0.1	2.3	0.1
H 1-56	-	-	-	-	2.6	0.0	2.6	0.0	2.6	0.0
H 1-58	1.9	0.1	1.6	0.0	1.2	0.1	1.1	0.0	1.2	0.0
H 1-59	-	-	-	-	1.3	0.1	1.2	0.1	1.2	0.1
H 1-60	-	-	-	-	2.2	0.1	1.8	0.2	1.5	0.2
H 1-61	2.2	0.1	2.2	0.1	1.8	0.1	1.6	0.1	1.5	0.1
H 1-62	-	-	-	-	2.5	0.2	2.3	0.1	2.4	0.2

**Table 4.** continued.

name	$P_Z$	$\sigma$	$P_Y$	$\sigma$	$P_J$	$\sigma$	$P_H$	$\sigma$	$P_{Ks}$	$\sigma$
H 1-63	-	-	-	-	1.4	0.1	1.2	0.1	1.2	0.1
H 1-64	2.7	0.2	2.8	0.4	2.7	0.0	2.5	0.2	2.4	0.2
H 1-66	-	-	-	-	-	-	1.7	0.2	-	-
H 2-1	-	-	-	-	2.4	0.1	2.0	0.2	2.0	0.1
H 2-10	2.7	0.1	2.6	0.1	2.5	0.0	2.3	0.0	2.2	0.0
H 2-13	4.6	0.3	4.4	0.6	3.1	0.3	3.0	0.1	2.7	0.5
H 2-20	-	-	-	-	2.2	0.0	2.0	0.0	2.2	0.0
H 2-23	3.5	0.2	2.8	0.9	2.0	0.9	1.3	0.1	1.7	0.6
H 2-24	2.4	1.3	2.1	1.0	1.5	0.0	2.2	0.2	3.6	0.3
H 2-25	2.3	0.0	2.0	0.0	1.9	0.0	1.8	0.0	2.2	0.0
H 2-26	1.6	n	-	-	-	-	1.2	n	1.3	0.1
H 2-27	3.0	0.0	2.5	0.0	2.0	0.1	1.4	0.1	2.0	0.1
H 2-29	1.3	n	1.0	0.1	0.9	n	-	-	-	-
H 2-35	-	-	-	-	1.3	0.2	0.9	n	-	-
H 2-36	-	-	-	-	1.4	0.4	1.0	0.1	-	-
H 2-37	2.8	0.1	2.4	0.2	2.7	0.1	1.5	0.3	2.4	0.4
H 2-39	-	-	-	-	2.0	0.6	1.3	0.1	2.4	0.6
H 2-40	-	-	-	-	2.1	0.0	1.8	0.0	1.8	0.0
H 2-41	-	-	-	-	-	-	1.2	0.1	1.2	0.2
H 2-42	-	-	-	-	2.6	0.0	2.5	0.0	2.4	0.3
H 2-45	2.2	0.0	2.2	0.0	2.2	0.0	2.1	0.0	2.2	0.0
H 2-46	2.8	0.2	2.9	0.2	2.6	0.1	2.3	0.1	1.8	0.1
Hb 5	-	-	-	-	5.0	0.3	4.2	0.4	4.0	0.2
He 2-84	3.3	0.4	2.7	0.0	2.6	0.0	2.5	0.1	2.7	0.3
He 2-90	3.4	0.3	2.7	0.3	3.2	0.4	3.2	0.1	3.3	0.5
He 2-96	2.4	0.1	2.4	0.0	2.3	0.0	2.1	0.0	2.2	0.1
He 2-106	2.4	0.3	3.2	0.6	5.6	0.8	7.9	n	8.4	1.9
He 2-117	4.1	0.0	4.1	0.1	4.1	0.0	3.9	0.0	3.9	0.1
He 2-133	3.8	0.3	3.8	0.2	3.4	0.0	3.3	0.0	3.2	0.0
He 2-140	3.2	0.0	3.1	0.0	3.1	0.1	3.0	0.0	3.1	0.1
He 2-142	4.5	0.1	4.3	0.3	4.5	0.0	3.7	0.6	3.9	0.9
He 2-143	2.8	0.0	2.8	0.1	2.5	0.0	2.3	0.0	2.4	0.1
He 2-153	-	-	-	-	-	-	-	-	1.1	n
He 2-250	4.2	0.0	3.9	0.1	3.9	0.0	3.7	n	4.0	0.2
He 2-262	3.7	0.2	3.9	0.0	2.9	0.6	3.6	0.4	3.1	0.7
Hf 2-1	-	-	-	-	2.6	0.1	1.8	0.6	2.3	0.4
Hf 2-2	1.7	0.1	1.4	0.1	1.3	0.1	0.9	0.1	1.0	0.1
IC 4673	3.3	0.1	3.1	0.1	2.2	0.8	2.1	0.1	-	-
IRAS18023-2513	2.6	0.4	3.3	0.2	3.5	0.8	3.2	0.2	4.3	0.5
JaFu 1	-	-	-	-	2.1	0.1	1.7	0.4	1.8	0.1
JaSt 2	-	-	1.5	n	-	-	-	-	-	-
JaSt 8	-	-	-	-	1.1	0.1	0.9	0.1	0.9	0.0
JaSt 16	-	-	-	-	3.0	0.1	2.6	0.1	2.5	0.6
JaSt 36	-	-	-	-	2.5	0.0	2.3	0.0	2.5	0.1

**Table 4.** continued.

name	$P_Z$	$\sigma$	$P_Y$	$\sigma$	$P_J$	$\sigma$	$P_H$	$\sigma$	$P_{Ks}$	$\sigma$
JaSt 46	-	-	-	-	2.5	0.0	2.3	0.4	2.5	0.0
JaSt 52	-	-	-	-	1.6	0.1	1.5	0.1	1.5	0.1
JaSt 54	-	-	-	-	1.4	0.1	1.8	0.3	2.4	0.2
JaSt 56	-	-	-	-	2.4	0.1	2.1	0.1	2.2	0.1
JaSt 63	-	-	-	-	0.9	n	2.8	0.0	-	-
JaSt 64	1.7	0.0	1.7	0.0	1.7	0.0	1.5	0.0	1.6	0.1
JaSt 65	2.4	0.5	2.4	0.2	2.5	0.7	2.0	0.1	2.1	0.4
JaSt 69	-	-	-	-	1.1	0.1	1.1	0.2	1.0	0.1
JaSt 71	-	-	-	-	2.0	0.0	1.9	0.0	2.0	0.0
JaSt 74	-	-	-	-	2.5	0.2	2.4	0.0	2.5	0.1
JaSt 75	-	-	-	-	2.0	0.1	1.9	0.1	1.9	0.2
JaSt 78	-	-	-	-	1.2	0.1	1.1	0.1	1.5	0.3
JaSt 79	1.8	0.1	1.7	0.1	1.8	0.3	2.9	0.8	3.0	1.1
JaSt 81	-	-	-	-	1.9	0.1	1.8	0.0	1.8	0.3
JaSt 95	-	-	-	-	1.1	0.0	1.1	0.1	1.3	0.2
K 5-5	2.3	0.6	2.0	0.1	1.6	0.0	1.5	0.0	1.5	0.0
K 5-6	-	-	-	-	2.1	0.2	2.5	0.4	2.4	0.3
K 5-8	1.8	0.1	1.7	0.0	1.8	0.1	2.2	0.2	1.7	0.6
K 5-10	1.9	0.5	2.0	0.3	1.9	0.3	2.3	0.3	1.1	0.1
K 5-18	-	-	-	-	1.0	0.1	-	-	-	-
K 5-19	2.5	0.0	-	-	-	-	1.7	0.2	2.2	0.3
K 5-20	3.0	0.4	2.7	0.1	2.5	0.0	2.1	0.1	2.9	0.3
K 6-7	2.9	n	2.8	n	2.2	0.4	1.6	0.3	1.7	0.5
KnFs 11	-	-	-	-	2.0	0.6	1.6	0.1	2.5	0.5
KnFs 12	-	-	-	-	1.7	0.0	1.3	0.0	2.0	0.9
KnFs 13	1.2	0.1	1.3	0.1	1.1	0.1	0.9	n	-	-
KnFs 14	-	-	-	-	1.1	0.0	1.2	0.1	1.1	0.1
KnFs 16	-	-	-	-	1.4	0.2	1.3	0.1	1.4	0.2
KnFs 19	-	-	-	-	1.8	0.3	1.4	0.4	0.9	n
Lo 10	-	-	-	-	-	-	1.1	0.0	1.5	0.5
M 1-19	-	-	-	-	2.7	0.0	2.5	0.0	2.6	0.1
M 1-26	-	-	-	-	3.3	0.5	3.0	0.4	3.0	0.3
M 1-28	-	-	-	-	0.9	n	-	-	1.0	n
M 1-30	-	-	-	-	3.3	0.0	3.2	0.0	3.2	0.1
M 1-31	-	-	-	-	2.3	0.0	2.3	0.1	2.3	0.1
M 1-34	-	-	-	-	-	-	2.2	n	2.0	n
M 1-37	2.6	0.1	2.4	0.0	2.6	0.2	2.5	0.2	2.5	0.3
M 1-38	2.5	0.0	2.5	0.2	2.8	0.4	1.8	0.4	2.3	0.3
M 2-10	-	-	-	-	2.5	0.0	2.2	0.0	2.5	0.1
M 2-11	-	-	-	-	2.9	0.6	1.7	0.1	2.1	0.3
M 2-14	3.1	0.4	3.0	0.4	2.3	0.0	2.1	0.0	2.1	0.0
M 2-16	3.1	0.1	2.9	0.1	2.8	0.1	2.6	0.1	2.5	0.1
M 2-18	2.3	0.2	2.4	0.5	2.3	0.4	2.0	0.1	2.0	0.1
M 2-19	-	-	-	-	1.5	0.1	1.3	0.1	1.4	0.2

**Table 4.** continued.

name	$P_Z$	$\sigma$	$P_Y$	$\sigma$	$P_J$	$\sigma$	$P_H$	$\sigma$	$P_{Ks}$	$\sigma$
M 2-21	2.4	0.0	2.3	0.0	4.5	0.0	2.4	0.0	2.9	0.5
M 2-22	-	-	-	-	3.6	0.9	2.5	1.6	2.9	1.2
M 2-23	2.4	0.3	2.0	0.2	2.1	0.2	2.0	0.4	1.9	0.5
M 2-24	-	-	-	-	1.9	0.0	1.9	0.0	2.4	0.1
M 2-25	-	-	-	-	1.6	0.4	-	-	-	-
M 2-26	2.0	0.0	2.2	0.1	1.6	0.3	1.0	0.1	1.1	0.1
M 2-27	-	-	-	-	2.3	0.1	2.2	0.1	2.2	0.1
M 2-28	3.0	0.0	2.6	0.0	3.0	0.1	1.9	0.0	2.0	0.3
M 2-30	-	-	-	-	2.7	0.0	2.7	0.0	2.6	0.0
M 2-31	3.2	0.0	3.2	0.1	3.1	0.0	3.0	0.0	2.9	0.0
M 2-32	-	-	-	-	2.8	0.2	2.6	0.2	2.7	0.1
M 2-33	-	-	-	-	2.9	0.0	2.9	0.0	3.1	0.1
M 2-34	1.4	0.0	1.3	0.0	1.3	0.0	1.3	0.0	1.3	0.0
M 2-36	-	-	-	-	3.9	0.4	3.1	0.3	3.3	0.3
M 2-37	-	-	-	-	1.9	0.1	1.7	0.1	2.2	0.8
M 2-38	-	-	-	-	-	-	1.3	0.2	-	-
M 2-39	-	-	-	-	2.2	0.2	1.6	0.3	1.5	0.1
M 2-41	1.6	0.4	1.6	0.7	1.1	0.0	2.0	0.7	1.1	n
M 2-42	-	-	-	-	3.4	0.1	3.3	0.2	3.3	0.1
M 3-7	4.1	1.4	2.1	0.0	2.1	n	-	-	2.6	1.3
M 3-10	3.4	0.2	3.3	0.1	3.3	0.1	2.6	0.2	2.4	0.0
M 3-14	4.6	0.0	4.2	0.6	4.7	0.0	3.2	0.3	3.7	0.9
M 3-16	3.4	0.3	3.2	0.3	3.2	0.1	2.9	0.4	2.9	0.3
M 3-17	2.6	0.1	2.3	0.0	2.3	0.0	2.1	0.1	2.3	0.0
M 3-19	-	-	-	-	-	-	-	-	2.7	n
M 3-20	2.9	0.0	2.8	0.0	2.5	0.0	2.5	0.0	2.5	0.1
M 3-22	-	-	-	-	2.7	n	1.6	n	1.9	0.4
M 3-26	-	-	-	-	1.3	0.3	1.1	0.0	1.0	n
M 3-38	-	-	-	-	1.9	0.2	1.6	0.0	1.6	0.0
M 3-41	3.2	0.3	3.0	0.2	3.2	0.1	2.3	0.6	2.2	0.5
M 3-42	5.3	1.1	2.0	n	-	-	-	-	1.4	0.4
M 3-43	-	-	-	-	3.2	0.3	3.2	0.3	3.2	0.3
M 3-45	3.3	0.8	3.5	0.5	3.5	0.1	2.3	0.2	2.7	0.2
M 3-46	1.9	0.3	1.5	0.3	1.9	0.2	1.2	n	1.5	0.1
M 3-51	-	-	-	-	1.6	0.1	1.8	0.1	1.6	0.3
M 4-6	3.3	0.5	2.6	0.0	-	-	-	-	2.8	0.4
M 4-7	4.2	0.8	3.3	0.9	4.0	1.4	2.8	0.5	4.3	1.4
MaC 1-11	2.8	0.2	2.9	0.2	2.6	0.1	2.6	0.2	2.5	0.1
MPA1157-6226	1.5	0.1	2.8	0.2	2.8	0.4	3.6	0.6	2.8	0.9
MPA1221-6413	2.5	0.0	2.2	0.0	2.4	0.0	2.2	0.0	2.2	0.1
MPA1235-6318	3.7	0.5	3.3	0.3	3.6	0.1	3.1	0.5	3.5	0.5
MPA1242-6459	2.6	0.2	2.6	0.4	2.4	0.0	2.3	0.0	2.3	0.0
MPA1243-6428	2.6	0.0	2.5	0.0	2.3	0.1	2.0	0.1	1.8	0.1
MPA1249-6414	1.8	0.1	2.0	0.1	1.9	0.1	1.7	0.1	1.9	0.2

**Table 4.** continued.

name	$P_Z$	$\sigma$	$P_Y$	$\sigma$	$P_J$	$\sigma$	$P_H$	$\sigma$	$P_{Ks}$	$\sigma$
MPA1309-6415	2.9	0.0	2.7	0.5	2.2	0.6	1.9	0.8	2.8	0.6
MPA1319-6418	1.9	0.0	1.9	0.0	1.9	0.0	1.9	0.0	2.2	0.3
MPA1326-6407	1.6	0.9	2.0	0.7	2.3	0.8	2.4	n	2.0	1.1
MPA1327-6031	1.8	n	1.8	n	1.7	n	1.9	n	1.7	0.1
MPA1346-6418	3.7	n	3.7	0.7	3.8	0.2	3.0	0.5	2.4	1.5
MPA1354-6337	3.6	0.0	3.5	0.0	3.4	0.1	3.4	0.1	3.2	0.3
MPA1428-6234	1.7	0.1	1.6	0.0	2.0	0.5	2.1	0.5	2.6	0.5
MPA1430-6251	2.7	0.3	3.1	0.3	3.3	0.3	2.8	0.3	3.0	0.9
MPA1439-5816	2.2	0.1	2.1	0.2	1.6	0.1	1.5	0.2	1.5	0.2
MPA1441-6114	3.4	0.6	2.9	0.0	2.8	0.0	2.7	0.1	2.7	0.1
MPA1517-5538	-	-	-	-	1.0	0.1	1.1	0.1	1.1	0.1
MPA1520-5517	1.2	n	1.4	n	3.4	n	1.7	n	2.2	0.9
MPA1522-5917	2.9	0.1	2.7	0.6	3.0	0.3	3.1	0.4	2.7	0.1
MPA1523-5710	5.3	n	3.9	1.9	3.1	1.0	2.7	0.5	3.7	1.1
MPA1530-5801	2.8	0.0	2.8	0.2	2.8	0.1	2.6	0.4	2.8	0.3
MPA1605-5319	3.0	0.1	3.0	0.1	3.1	0.2	3.0	0.3	2.8	0.1
MPA1606-5407	2.3	0.1	2.1	0.1	1.9	0.2	1.6	0.0	1.6	0.1
MPA1618-5147	1.8	0.1	2.2	0.4	1.6	0.0	1.2	0.1	1.5	0.2
MPA1635-4458	2.3	0.1	2.1	0.4	1.9	0.4	1.6	0.0	1.6	0.0
MPA1650-4747	3.1	0.5	3.3	0.4	3.3	0.2	3.4	0.1	3.5	0.2
MPA1703-4450	2.3	0.0	2.4	0.1	2.2	0.0	2.1	0.0	2.3	0.2
MPA1711-3112	-	-	-	-	2.9	0.4	2.4	0.5	2.2	0.5
MPA1713-4015	-	-	-	-	2.7	0.0	2.4	0.0	2.2	0.0
MPA1717-3945	-	-	-	-	2.5	0.0	2.5	0.0	2.7	0.8
MPA1719-3247	-	-	4.7	0.2	-	-	-	-	-	-
MPA1725-3033	1.7	0.4	1.7	0.3	2.4	0.1	2.0	0.1	1.7	0.4
MPA1728-3132	-	-	-	-	2.2	0.0	2.1	0.0	2.2	0.0
MPA1729-3016	2.0	0.3	1.8	0.3	1.5	0.0	1.5	0.0	1.3	0.1
MPA1736-3717	-	-	-	-	1.2	0.1	-	-	1.5	n
MPA1737-3837	-	-	-	-	3.7	0.7	2.9	0.5	2.6	0.8
MPA1739-2648	1.9	0.0	1.8	0.1	1.3	0.1	1.1	0.0	1.1	0.0
MPA1742-2613	2.0	0.3	1.7	0.2	1.2	0.0	1.2	0.1	1.1	0.1
MPA1744-3444	1.8	0.1	2.0	n	2.3	0.1	2.0	0.2	2.2	0.3
MPA1747-2649	-	-	-	-	1.6	0.0	1.5	0.0	1.6	0.1
MPA1751-2223	-	-	-	-	1.5	0.1	1.7	0.3	1.6	0.2
MPA1751-2838	-	-	-	-	1.8	0.0	1.6	0.1	1.7	0.1
MPA1751-3339	1.4	0.1	1.3	0.1	1.2	0.1	1.2	0.1	1.3	0.1
MPA1755-2212	2.4	0.6	2.1	0.7	1.6	0.0	1.5	0.0	1.5	0.1
MPA1755-2741	-	-	-	-	1.2	0.0	1.4	0.1	1.3	0.1
MPA1757-3410	-	-	-	-	1.4	0.2	1.4	0.2	1.1	0.2
MPA1800-3023	-	-	1.1	0.1	-	-	-	-	-	-
MPA1815-2113	3.0	0.1	2.8	0.1	2.9	0.0	2.5	0.0	2.9	0.1
NGC 6644	3.5	0.1	3.3	0.0	2.6	0.1	2.2	0.0	2.3	0.2
Pe 1-7	2.2	0.0	2.1	0.1	2.0	0.0	2.3	0.0	2.2	0.2

**Table 4.** continued.

name	$P_Z$	$\sigma$	$P_Y$	$\sigma$	$P_J$	$\sigma$	$P_H$	$\sigma$	$P_{Ks}$	$\sigma$
Pe 1-9	1.6	0.1	1.4	0.1	1.2	0.0	1.1	0.0	1.1	0.1
Pe 2-8	2.1	0.0	2.1	0.0	2.2	0.2	2.2	0.3	2.3	0.3
Pe 2-10	-	-	-	-	1.2	0.0	1.3	0.1	1.3	0.1
PHR1202-6112	-	-	-	-	-	-	-	-	1.2	0.2
PHR1213-6344	1.5	0.1	1.4	0.1	1.6	0.4	1.4	0.2	1.4	0.1
PHR1223-6236	1.5	n	1.5	0.1	1.3	0.1	1.2	0.1	1.3	0.1
PHR1250-6346	1.1	n	0.9	n	1.2	0.2	1.2	0.0	1.1	0.1
PHR1257-6052	0.9	n	1.2	0.2	1.2	0.2	1.1	0.1	1.3	0.2
PHR1318-6358	1.3	0.1	1.6	0.3	1.5	0.3	1.3	0.1	1.2	0.1
PHR1324-6418	1.7	0.2	1.6	0.2	1.1	0.1	1.1	0.1	1.2	0.1
PHR1324-6448	2.0	0.4	1.9	0.4	1.5	0.1	1.4	0.1	1.3	0.1
PHR1327-6032	1.8	0.2	1.9	0.3	1.8	0.1	2.1	0.2	1.4	0.4
PHR1335-6015	2.1	0.0	1.7	0.0	1.6	n	1.8	0.1	1.5	0.3
PHR1341-6427	-	-	-	-	-	-	1.1	0.0	2.0	0.3
PHR1408-6229	2.4	0.6	2.1	0.4	2.5	0.5	2.6	0.6	1.8	0.8
PHR1420-5933	2.6	0.2	3.3	0.3	1.1	0.1	2.1	0.6	2.4	0.8
PHR1438-6140	1.7	n	1.1	n	1.4	0.0	1.0	n	1.3	0.1
PHR1447-6127	-	-	-	-	1.3	n	1.3	0.0	1.1	0.1
PHR1453-5714	2.1	0.7	2.1	0.7	1.2	0.0	1.2	0.1	1.2	0.2
PHR1507-5925	2.1	0.1	2.1	0.1	2.0	0.1	1.9	0.4	2.0	0.2
PHR1539-5727	2.3	0.7	2.0	0.5	1.4	0.1	1.4	0.0	1.4	0.1
PHR1551-5653	1.7	0.0	1.5	0.0	1.4	0.1	1.2	0.0	1.2	0.1
PHR1552-5254	1.0	n	1.4	0.3	1.3	0.3	1.2	0.2	1.3	0.3
PHR1557-5128	1.6	0.3	1.6	0.1	1.6	0.1	1.8	0.5	1.4	0.2
PHR1619-4907	-	-	-	-	-	-	1.1	n	0.9	0.0
PHR1633-4650	-	-	1.5	0.1	1.8	0.0	1.7	0.1	1.6	0.2
PHR1634-4628	1.4	0.1	1.4	0.0	1.3	0.0	1.3	0.0	1.2	0.0
PHR1639-4516	-	-	1.5	n	1.0	0.1	1.0	0.1	1.0	0.1
PHR1704-3819	1.9	0.1	1.7	0.1	1.5	0.3	1.4	0.2	1.5	0.2
PHR1707-4309	2.1	0.3	1.9	0.3	1.6	0.0	1.4	0.1	1.7	0.3
PHR1709-3931	1.3	0.0	1.3	0.0	1.3	0.1	1.3	0.2	1.3	0.2
PHR1712-3452	1.6	0.0	1.7	0.0	1.7	0.1	1.5	0.1	1.6	0.1
PHR1714-4006	-	-	-	-	2.3	0.3	2.3	0.4	2.5	0.3
PHR1735-2527	-	-	-	-	1.0	n	-	-	1.1	n
PHR1752-3244	1.1	0.1	1.1	0.1	1.0	0.1	1.0	0.1	0.9	0.0
PHR1801-2522	-	-	-	-	4.2	0.4	4.6	0.3	4.1	0.4
PHR1802-2637	1.8	0.0	1.8	0.0	1.1	0.1	1.0	0.1	1.0	0.1
PHR1804-2653	1.5	0.4	1.9	0.2	1.9	0.1	1.9	0.1	1.2	0.2
PHR1804-2913	2.3	0.0	2.0	0.1	1.7	0.5	1.6	0.4	1.4	0.3
PN 1231-6401	2.2	0.2	2.6	0.0	2.4	0.0	2.2	0.0	1.9	0.1
PN 1412-5947	2.8	0.2	2.7	0.2	2.3	0.1	2.1	0.1	2.0	0.2
PN 1434-5858	2.7	0.2	2.3	0.0	1.8	0.1	1.7	0.1	1.8	0.2
PN 1557-5445	2.1	0.0	2.1	0.1	1.7	0.0	1.5	0.0	1.5	0.1
PN 1600-5041	1.7	0.2	1.5	0.1	1.4	0.2	1.2	0.1	1.3	0.1

**Table 4.** continued.

name	$P_Z$	$\sigma$	$P_Y$	$\sigma$	$P_J$	$\sigma$	$P_H$	$\sigma$	$P_{Ks}$	$\sigma$
PN 1652-4341	4.1	0.0	3.5	0.6	3.7	0.0	3.7	0.0	3.8	0.3
PN 1708-4227	2.3	0.1	2.2	0.1	1.8	0.1	1.6	0.1	1.6	0.0
PPA1704-3824	3.7	0.3	3.2	0.9	3.2	0.9	3.3	0.9	4.1	0.8
PPA1705-3748	2.8	0.0	3.1	0.0	3.0	0.2	2.6	0.3	2.8	0.4
PPA1715-3313	-	-	2.4	0.3	-	-	-	-	-	-
PPA1718-3315	1.8	0.2	1.8	0.1	-	-	-	-	-	-
PPA1721-3149	3.2	0.0	3.4	0.1	-	-	-	-	-	-
PPA1722-3139	2.9	0.0	2.8	0.1	-	-	-	-	-	-
PPA1722-3317	3.1	0.3	2.8	0.1	2.9	0.0	1.5	0.1	2.1	0.8
PPA1723-3038	-	-	-	-	-	-	-	-	2.5	n
PPA1724-3043	2.5	0.4	2.4	0.3	1.8	0.0	1.7	0.1	1.6	0.1
PPA1725-3216	2.0	0.2	2.6	0.8	-	-	-	-	-	-
PPA1726-3045	3.2	0.7	3.4	0.5	3.5	0.0	3.4	0.3	3.0	0.4
PPA1729-2611	-	-	-	-	3.8	0.0	3.6	0.1	3.7	0.1
PPA1730-2621	-	-	-	-	1.5	0.0	1.3	0.0	1.7	0.2
PPA1734-3004	-	-	-	-	1.5	0.0	1.4	0.0	1.7	0.3
PPA1734-3102	-	-	-	-	2.5	0.2	2.7	0.2	2.7	0.1
PPA1735-2809	3.2	0.1	2.6	0.2	-	-	-	-	-	-
PPA1737-3414	-	-	-	-	1.6	0.3	1.3	0.2	2.0	0.2
PPA1737-3650	-	-	-	-	1.6	0.0	1.5	0.0	1.7	0.0
PPA1738-3753	-	-	-	-	1.8	0.0	1.8	0.0	1.8	0.0
PPA1740-2708	1.2	0.1	-	-	1.2	0.1	-	-	1.3	0.3
PPA1741-2332	1.0	0.1	1.0	0.1	0.9	0.1	0.9	0.1	1.0	0.1
PPA1741-3405	1.2	n	1.8	0.5	3.1	0.4	1.6	0.1	1.6	0.4
PPA1743-3315	3.7	0.8	3.7	0.8	3.3	0.4	1.4	0.2	2.8	0.2
PPA1746-3454	1.6	0.0	1.5	0.0	1.5	0.1	1.2	0.1	1.2	0.0
PPA1747-3215	2.0	0.2	2.4	0.0	2.5	0.0	2.2	0.0	2.0	0.6
PPA1750-3152	-	-	1.1	n	-	-	-	-	-	-
PPA1756-2311	1.9	n	-	-	1.4	0.0	1.6	0.3	-	-
PPA1800-2904	1.1	n	1.1	n	-	-	-	-	1.5	n
PPA1801-2553	2.7	0.0	2.6	0.0	2.8	0.7	2.7	0.1	2.7	0.1
PPA1803-2516	2.1	0.1	1.8	0.1	1.2	0.0	1.6	0.1	1.3	0.1
PPA1803-2826	2.8	0.2	2.1	0.3	2.3	0.3	1.6	0.1	1.4	0.2
PPA1809-3233	-	-	-	-	1.6	0.3	1.3	0.1	1.1	0.1
PPA1813-2233	2.1	0.7	2.9	0.1	2.2	0.7	1.7	0.7	1.6	0.7
PPA1831-2356	-	-	-	-	1.3	0.5	1.6	0.2	1.4	0.3
Sa 2-215	-	-	-	-	1.9	0.1	2.1	0.1	1.9	0.1
Sa 3-92	2.7	0.8	2.3	0.9	-	-	2.1	n	1.9	0.4
Sa 3-104	1.7	0.0	1.6	0.1	1.9	0.3	1.6	0.1	1.6	0.0
SAWI 5	-	-	-	-	1.4	0.1	1.2	0.1	1.4	0.1
SAWI 7	-	-	-	-	1.5	0.2	1.4	0.1	1.5	0.1
SB 1	2.5	0.2	2.5	0.0	2.2	0.2	-	-	-	-
SB 4	1.4	0.1	1.3	0.1	1.3	0.1	1.1	0.1	1.0	0.1
SB 5	-	-	-	-	1.2	0.1	1.1	0.0	1.1	0.0

**Table 4.** continued.

name	P <sub>Z</sub>	$\sigma$	P <sub>Y</sub>	$\sigma$	P <sub>J</sub>	$\sigma$	P <sub>H</sub>	$\sigma$	P <sub>Ks</sub>	$\sigma$
SB 9	-	-	1.0	n	1.2	n	1.0	n	-	-
SB 12	-	-	-	-	1.7	0.0	1.8	0.0	1.5	0.1
SB 14	-	-	-	-	1.3	0.1	1.1	0.2	1.0	0.1
SB 16	2.5	0.0	2.5	0.0	2.5	0.0	2.1	0.2	1.5	0.2
SB 37	-	-	-	-	3.7	0.7	3.6	0.6	3.3	0.4
SB 38	1.9	0.1	1.8	0.1	1.7	0.1	1.6	0.1	1.3	0.1
SB 39	2.2	0.3	2.1	0.5	1.4	0.1	1.1	0.1	1.2	0.2
SB 49	3.0	0.1	2.9	0.1	1.7	0.0	1.5	0.1	1.5	0.1
SB 51	-	-	-	-	1.6	0.4	1.3	0.2	1.4	0.2
SB 54	-	-	-	-	1.6	0.2	1.3	0.2	1.3	0.2
SB 55	1.6	0.0	1.7	0.1	1.3	0.1	1.1	0.0	1.1	0.1
SB 56	-	-	-	-	2.2	0.7	1.9	0.4	1.7	0.3
SrWe 2	-	-	-	-	1.5	0.0	1.4	0.1	1.4	0.1
SwSt 1	3.9	0.9	3.1	0.9	2.7	0.5	2.2	0.2	2.5	0.2
Ta 137	1.9	n	1.0	n	-	-	-	-	-	-
Ta 140	-	-	-	-	1.4	0.0	1.5	0.1	1.7	0.2
Ta 1567	-	-	-	-	0.9	n	1.0	0.1	-	-
Ta 2337	-	-	-	-	1.3	0.1	1.1	0.0	1.1	0.0
Th 3-4	2.0	0.0	2.6	0.6	-	-	-	-	-	-
Th 3-6	3.1	0.0	3.2	0.1	-	-	-	-	-	-
Th 3-10	3.4	0.1	3.6	0.4	3.7	0.0	3.7	0.0	3.1	0.6
Th 3-11	2.5	n	2.9	0.7	-	-	-	-	-	-
Th 3-12	2.4	0.2	2.3	0.3	2.5	0.1	2.1	0.1	1.7	0.2
Th 3-13	2.5	0.3	2.2	0.2	2.0	0.1	1.9	0.0	1.6	0.0
Th 3-14	-	-	-	-	1.3	0.1	1.4	0.1	1.4	0.1
Th 3-15	-	-	-	-	2.3	0.4	1.9	0.2	2.0	0.3
Th 3-19	2.0	0.3	1.9	0.3	1.9	0.3	1.5	0.1	1.4	0.1
Th 3-23	3.4	0.1	3.5	0.1	-	-	-	-	3.7	0.0
Th 3-25	3.5	0.0	3.7	0.0	-	-	-	-	-	-
Th 3-27	-	-	-	-	2.6	0.4	1.1	0.0	2.2	0.9
Th 3-33	2.0	0.1	1.8	0.0	-	-	-	-	-	-
Th 3-35	-	-	-	-	2.1	0.5	2.5	0.1	2.4	0.2
Th 3-55	-	-	-	-	2.3	0.1	2.1	0.0	2.4	0.0
Th 4-3	1.9	0.1	1.7	0.0	1.2	0.1	1.3	0.1	1.4	0.1
Th 4-5	2.2	0.6	3.7	1.4	1.3	n	5.4	n	-	-
Th 4-6	2.5	0.5	2.5	0.7	1.9	0.1	1.6	0.0	1.6	0.0
Th 4-9	1.6	0.0	1.6	0.0	1.3	0.1	1.2	0.1	1.3	0.2
VB 2	2.7	0.7	2.2	0.4	1.6	0.1	1.4	0.1	1.4	0.1
VB 3	2.0	0.2	-	-	1.8	0.2	1.4	0.2	1.4	0.3
VBRC 7	-	-	-	-	-	-	1.0	n	-	-
Vd 1-8	2.4	0.1	2.3	0.0	2.2	0.1	2.1	0.1	2.0	0.1
Vd 1-9	2.5	0.3	2.4	0.2	2.1	0.0	2.0	0.0	2.1	0.1
Vy 2-1	-	-	-	-	3.2	0.0	3.1	0.1	3.0	0.0
WeKG 2	1.3	0.1	1.3	0.1	1.1	0.0	1.1	0.0	1.3	0.2

**Table 4.** continued.

name	$P_Z$	$\sigma$	$P_Y$	$\sigma$	$P_J$	$\sigma$	$P_H$	$\sigma$	$P_{Ks}$	$\sigma$
WeKG 3	1.3	0.1	1.2	0.1	1.1	0.0	1.1	0.0	1.4	0.2

**Table 5.** Planetary nebulae that were not measured.

name	PN G	$\alpha$ (2000)	$\delta$ (2000)	status
JaSt 93	000.1–01.9	17 53 24.43	−29 49 47.7	N/D
Bl 3-10	000.1–02.3	17 55 20.48	−29 57 33.4	N/D
K 6-8	000.2+01.7	17 39 39.253	−27 47 23.56	N/D
PHR1752-2930	000.3–01.6	17 52 52.20	−29 30 00.1	N/D
JaSt 86	000.3–01.6	17 52 52.20	−29 30 00.1	N/D
Sa 3-117	000.3–02.8	17 57 43.367	−30 02 29.91	N/D
M 3-47	000.3–04.6	18 05 02.695	−30 58 17.39	ext
M 2-20	000.4–02.9	17 58 19.337	−30 00 39.32	N/D
JaSt 96	000.5–01.7	17 25 03.470	−31 28 38.50	N/D
Ae 2-Q	000.5–03.1	17 59 15.585	−30 02 47.15	N/D
SB 2	000.5–05.3	18 08 34.7	−31 06 52	N/D
JaSt 77	000.6–01.0	17 51 11.504	−28 56 26.16	N/D
KnFs 1	000.6–01.3	17 52 35.87	−29 06 38.6	N/D
SB 3	000.7–06.1	18 12 14.48	−31 19 58.0	N/D
M 2-35	000.7–07.4	18 17 37.195	−31 56 46.86	ext
JaSt 38	000.8+01.3	17 42 32.674	−27 33 08.82	N/D
JaSt 44	000.9+01.1	17 43 23.305	−27 34 03.57	N/D
PHR1804-3016	000.9–04.2	18 04 48.1	−30 16 49	N/D
M 3-23	000.9–04.8	18 07 06.148	−30 34 16.96	ext
JaSt 41	001.0+01.3	17 42 49.96	−27 21 19.7	N/D
K 1-4	001.0+01.9	17 40 27.366	−27 01 02.91	N/D
JaSt 89	001.3–01.0	17 53 06.57	−28 18 09.2	N/D
SAWI 1	001.4–03.4	18 02 25.85	−29 25 05.4	N/D
K 6-17	001.5–00.7	17 52 08.717	−28 02 16.56	N/D
JaSt 55	001.6+00.9	17 45 37.36	−27 01 18.4	N/D
K 6-10	001.6+01.5	17 43 16.950	−26 44 17.54	N/D
Bl Q	001.6–01.3	17 54 34.94	−28 12 43.3	N/D
SB 6	001.6–05.9	18 13 15.842	−30 25 58.49	N/D
H 1-45	002.0–02.0	17 58 21.87	−28 14 52.3	ext
KnFs 2	002.2–02.5	18 00 59.92	−28 16 19.8	N/D
PHR1808-2913	002.2–04.3	18 08 06.42	−29 13 15.7	N/D
Cn 1-5	002.2–09.4	18 29 11.675	−31 29 58.81	ext
PHR1744-2603	002.3+01.7	17 44 35.4	−26 03 36	N/D
Ta 5	002.3+02.2	17 42 30.10	−25 45 28.7	N/D
PPA1741-2538	002.3+02.4	17 41 48.4	−25 38 18	N/D
Sa 3-115	002.4–03.2	18 04 05.438	−28 27 50.90	N/D
Pe 2-11	002.5–01.7	17 58 31.27	−27 37 05.8	S/D
Ta 1580	002.6+02.1	17 43 39.442	−25 36 42.51	N/D
PPA1745-2542	002.7+01.7	17 45 18.9	−25 42 05	N/D
M 1-42	002.7–04.8	18 11 05.07	−28 58 58.5	ext
Pe 2-12	002.8–02.2	18 01 10.300	−27 38 19.88	S/D
Hb 4	003.1+02.9	17 41 52.763	−24 42 08.07	ext
K 5-7	003.1+04.1	17 37 20.167	−24 03 27.84	N/D
SB 7	003.3–06.1	18 17 46.363	−29 06 07.52	N/D

**Table 5.** continued.

name	PN G	$\alpha$ (2000)	$\delta$ (2000)	status
MPA1748-2511	003.5+01.3	17 48 41.629	-25 11 33.37	ext
NGC 6565	003.5-04.6	18 11 52.470	-28 10 42.27	ext
PHR1759-2630	003.6-01.3	17 59 12.09	-26 30 24.8	ext
Ta 2111	003.9+01.6	17 48 28.465	-24 41 25.07	N/D
M 1-35	003.9-02.3	18 03 39.30	-26 43 33.9	ext
KnFs 7	003.9-03.1	18 06 50.05	-27 06 16.09	S/D
M 2-29	004.0-03.0	18 06 40.862	-26 54 55.95	S/D
Pe 1-12	004.0-05.8	18 17 42.37	-28 17 16.5	N/D
KnFs 10	004.2-03.2	18 08 01.312	-26 54 01.52	S/D
SB 8	004.2-05.2	18 15 50.3	-27 49 00	N/D
H 1-53	004.3-02.6	18 05 57.43	-26 29 42.0	S/D
MPA1748-2402	004.5+02.0	17 48 21.26	-24 02 14.0	N/D
SB 10	004.7-05.5	18 18 06.9	-27 31 35	N/D
M 1-25	004.9+04.9	17 38 30.32	-22 08 38.8	ext
H 1-27	005.0+04.4	17 40 17.95	-22 19 18.0	S/D
M 3-13	005.2+04.2	17 41 36.62	-22 13 03.0	S/D
SB 11	005.2-05.9	18 20 44.7	-27 15 48	N/D
M 3-24	005.5-02.5	18 07 53.914	-25 24 02.71	ext
H 2-44	005.5-04.0	18 13 40.45	-26 08 38.3	N/D
NGC 6620	005.8-06.1	18 22 54.17	-26 49 17.1	ext
KnFs 15	006.2-03.7	18 14 19.324	-25 20 51.22	N/D
H 2-18	006.3+04.4	17 43 28.751	-21 09 51.29	S/D
Pe 2-13	006.4-04.6	18 18 13.41	-25 38 10.4	N/D
M 1-41	006.7-02.2	18 09 29.902	-24 12 23.46	N/D
Th 4-7	006.8+02.3	17 52 22.569	-21 51 13.43	ext
M 3-15	006.8+04.1	17 45 31.74	-20 58 01.8	ext
Hb 6	007.2+01.8	17 55 07.023	-21 44 39.98	ext
Th 4-1	007.5+04.3	17 46 20.82	-20 13 48.3	S/D
H 1-65	007.8-04.4	18 20 08.85	-24 15 05.0	S/D
NGC 6445	008.0+03.9	17 49 15.21	-20 00 34.5	ext
M 1-40	008.3-01.1	18 08 25.994	-22 16 53.25	ext
He 2-406	008.6-07.0	18 31 52.845	-24 46 16.55	ext
PHR1751-1925	008.8+03.8	17 51 08.7	-19 25 47	N/D
NGC 6629	009.4-05.0	18 25 42.458	-23 12 10.23	ext
M 3-32	009.4-09.8	18 44 43.03	-25 21 34.8	ext
H 1-67	009.8-04.6	18 25 04.976	-22 34 52.64	ext
IRAS18333-2357	009.8-07.5	18 36 22.85	-23 55 19.5	N/D
BMP1145-6328	295.6-01.5	11 45 09.4	-63 28 54	N/D
PHR1206-6122	297.5+01.0	12 06 25.5	-61 22 44	N/D
PHR1203-6403	297.6-01.6	12 03 12.4	-64 03 41	N/D
PHR1212-6043	298.2+01.8	12 12 48.4	-60 43 15	N/D
He 2-76	298.2-01.7	12 08.4	-64 12	ext
PHR1216-6039	298.6+01.9	12 16 09.1	-60 39 32	N/D
PHR1212-6407	298.6-01.5	12 12 28.0	-64 07 11	N/D

**Table 5.** continued.

name	PN G	$\alpha$ (2000)	$\delta$ (2000)	status
He 2-81	299.8-01.3	12 23.0	-64 02	ext
He 2-83	300.2+00.6	12 28.7	-62 06	ext
He 2-85	300.5-01.1	12 30.1	-63 53	ext
He 2-86	300.7-02.0	12 30.5	-64 53	ext
MPA1239-6048	301.5+02.0	12 39 46.3	-60 48 17	ext
PHR1244-6231	302.1+00.3	12 44 28.5	-62 31 19	N/D
PHR1246-6324	302.3-00.5	12 46 26.5	-63 24 28	ext
VBRC 4	302.6-00.9	12 48.5	-63 50	N/D
PHR1309-6457	304.7-02.1	13 09 01.7	-64 57 18	N/D
MPA1315-6338	305.6-00.9	13 15 30.4	-63 38 43	ext
Th 2-A	306.4-00.6	13 22.5	-63 21	N/D
BMP1322-6330	306.4-00.8	13 22 55.4	-63 30 34	N/D
MPA1324-6320	306.6-00.7	13 24 16.8	-63 20 06	N/D
MPA1330-6438	307.0-02.0	13 30 11.0	-64 38 27	N/D
PHR1326-6103	307.1+01.5	13 26 21.7	-61 03 08	N/D
PHR1332-6412	307.3-01.6	13 32 05.7	-64 12 30	N/D
MPA1337-6258	308.1-00.5	13 37 54.9	-62 58 54	ext
VBRC 5	309.2+01.3	13 44.0	-60 50	N/D
Vo 4	310.4+01.3	13 53.4	-60 34	ext
PHR1408-6106	312.1+00.3	14 08 51.7	-61 06 27	N/D
He 2-107	312.6-01.8	14 18.7	-63 07	ext
BMP1423-5923	314.4+01.3	14 23 59.7	-59 23 38	ext
PN 1417-5824	314.4+02.2	14 21.3	-58 39	ext
PHR1432-6138	314.5-01.0	14 32 05.0	-61 38 42	N/D
He 2-111	315.0-00.3	14 33.3	-60 50	ext
LoTr 9	315.7-01.2	14 41.3	-61 20	N/D
PHR1437-5949	315.9+00.3	14 37 53.2	-59 49 25	N/D
LoTr 10	316.3-01.3	14 46.3	-61 14	N/D
MPA1440-5802	316.9+01.8	14 40 27.4	-58 02 19	ext
He 2-114	318.3-02.0	15 04.2	-60 54	ext
PHR1457-5812	318.9+00.7	14 57 35.7	-58 12 09	ext
He 2-120	321.8+01.9	15 12.0	-55 40	ext
BMP1525-5823	322.0-01.3	15 25 59.4	-58 23 02	ext
MPA1525-5528	323.5+01.1	15 25 06.1	-55 28 22	N/D
MPA1539-5709	324.1-01.3	15 39 10.6	-57 09 51	N/D
PHR1548-5629	325.5-01.6	15 48 21.3	-56 29 56	N/D
FP1550-5639	325.6-01.8	15 50 04.6	-56 39 13	N/D
BMP1533-5319	325.7+02.2	15 33 20.6	-53 19 01	ext
MPA1541-5243	327.1+01.9	15 41 29.5	-52 43 49	ext
MPA1559-5552	327.1-02.0	15 59 11.1	-55 52 18	N/D
PHR1547-5214	328.0+01.8	15 47 09.6	-52 14 44	N/D
Sp 1	329.0+01.9	15 51.6	-51 31	ext
HeFa 1	329.5-02.2	16 12.5	-54 24	S/D
BMP1613-5406	329.8-02.1	16 13 02.0	-54 06 32	N/D

**Table 5.** continued.

name	PN G	$\alpha$ (2000)	$\delta$ (2000)	status
PHR1616-5324	330.7-02.0	16 16 54.2	-53 24 40	N/D
PHR1603-5016	331.3+01.6	16 03 53.7	-50 16 52	ext
He 2-145	331.4+00.5	16 09.0	-51 02	ext
Mz 3	331.7-01.0	16 17.2	-51 59	ext
PHR1626-5216	332.5-02.2	16 26 24.2	-52 16 58	N/D
He 2-152	333.4+01.1	16 15.3	-49 13	ext
PHR1619-4914	333.9+00.6	16 19 40.1	-49 14 00	ext
MmWe 1-6	334.3-01.4	16 31.1	-50 26	ext
He 2-169	335.4-01.1	16 34.3	-49 21	ext
PHR1637-4957	335.4-01.9	16 37 44.9	-49 57 50	ext
Pe 1-6	336.2+01.9	16 23.9	-46 42	ext
BMP1636-4529	338.6+01.1	16 36 58.7	-45 29 29	N/D
MPA1657-4447	341.5-01.1	16 57 13.3	-44 47 18	N/D
PHR1702-4443	342.0-01.7	17 02 04.3	-44 43 20	N/D
H 1-3	342.7+00.7	16 53.5	-42 39	N/D
He 2-198	342.9-02.0	17 06.4	-44 13	ext
HtTr 5	343.3-00.6	17 01.5	-43 06	N/D
PHR1653-4143	343.5+01.2	16 53 55.3	-41 44 00	N/D
H 1-5	343.9+00.8	16 57.4	-41 38	ext
H 1-6	344.2-01.2	17 07.0	-42 41	ext
H 1-7	345.2-01.2	17 10.4	-41 53	ext
IC 4637	345.4+00.1	17 05.2	-40 53	ext
MPA1715-3903	348.0-00.3	17 15 16.1	-39 03 48	N/D
PHR1710-3732	348.7+01.3	17 10 12.3	-37 32 51	N/D
PHR1724-3859	349.1-01.7	17 24 30.7	-38 59 44	N/D
NGC 6337	349.3-01.1	17 22.2	-38 29	ext
NGC 6302	349.5+01.0	17 13.8	-37 06	ext
MPA1727-3851	349.6-02.1	17 27 36.8	-38 51 09	N/D
H 1-26	350.1-03.9	17 36 29.90	-39 21 56.8	ext
H 1-28	350.5-05.0	17 42 54.066	-39 36 24.04	ext
PPA1734-3817	350.8-03.0	17 34 52.8	-38 17 19	N/D
SB 33	351.2-06.3	17 50 27.700	-39 40 17.40	N/D
SB 34	351.5-06.5	17 52 09.386	-39 32 14.52	S/D
H 1-37	351.6-06.2	17 50 44.569	-39 17 25.98	ext
SB 35	351.7-06.6	17 53 02.87	-39 24 08.9	S/D
SB 36	352.0-06.7	17 54 20.83	-39 10 37.9	S/D
H 1-12	352.6+00.1	17 26 24.258	-35 01 41.88	ext
H 1-13	352.8-00.2	17 28 27.46	-35 07 31.8	ext
Fg 3	352.9-07.5	18 00 11.82	-38 49 52.6	S/D
H 1-38	353.2-05.2	17 50 45.216	-37 23 54.18	N/D
PPA1738-3546	353.3-02.2	17 38 16.2	-35 46 27	N/D
PPA1740-3551	353.5-02.6	17 40 21.4	-35 51 31	N/D
JaFu 2	353.5-05.0	17 50 11.1	-37 03 27	N/D
H 1-52	354.4-07.8	18 04 57.594	-37 38 07.92	S/D

**Table 5.** continued.

name	PN G	$\alpha$ (2000)	$\delta$ (2000)	status
PHR1722-3210	354.5+02.4	17 22 11.7	-32 10 45	N/D
PPA1740-3437	354.5-02.0a	17 40 30.5	-34 37 17	N/D
Ta 139	354.6+04.9	17 12 53.539	-30 40 05.70	N/D
SB 40	354.7-07.2	18 02 55.69	-37 08 13.1	S/D
H 1-31	355.1-02.9	17 45 32.104	-34 33 55.32	N/D
M 3-21	355.1-06.9	18 02 32.33	-36 39 11.3	S/D
SB 42	355.3-07.5	18 05 52.556	-36 45 37.40	S/D
Ta 138	355.4+02.3	17 25 03.470	-31 28 38.50	ext
PHR1740-3324	355.6-01.4	17 40 54.9	-33 24 18	N/D
PHR1721-3027	355.8+03.5	17 21 31.7	-30 27 20	N/D
SB 43	355.8-08.7	18 12 23.684	-36 52 53.72	N/D
PPA1741-3302	356.0-01.4	17 41 33.4	-33 02 15	N/D
SB 44	356.0-07.4A	18 07 07.953	-36 02 45.64	S/D
SB 45	356.0-07.4B	18 06 52.495	-36 06 42.82	S/D
PPA1747-3341	356.1-02.7	17 47 04.8	-33 41 03	N/D
SB 46	356.1-08.6	18 12 39.873	-36 31 49.16	N/D
PPA1751-3401	356.2-03.6	17 51 06.9	-34 01 41	N/D
M 3-49	356.3-06.2	18 02 32.06	-35 13 14.3	S/D
SB 47	356.3-07.3	18 07 21.472	-35 45 44.04	N/D
SB 48	356.4-06.8	18 05 14.396	-35 28 07.54	S/D
H 1-57	356.6-07.8	18 09 49.240	-35 44 13.32	S/D
H 1-51	356.7-06.4	18 04 29.304	-34 58 00.98	S/D
M 4-4	357.0+02.4	17 28 50.29	-30 07 45.1	N/D
Th 3-24	357.1+01.9	17 30 51.354	-30 17 12.49	N/D
TaJu 18	357.1+04.4	17 21 37.90	-28 55 13.9	N/D
M 3-50	357.1-06.1	18 04 05.183	-34 28 37.39	S/D
H 1-42	357.2-04.5	17 57 25.17	-33 35 42.9	ext
H 2-7	357.3+04.0	17 23 24.936	-28 59 06.05	ext
SB 50	357.3-06.5	18 06 08.301	-34 33 30.72	S/D
PPA1749-3216	357.5-02.4	17 49 37.82	-32 16 27.9	N/D
PPA1802-3350	357.5-05.5	18 02 23.8	-33 50 48	N/D
Pe 1-11	358.0-05.1	18 01 42.89	-33 15 28.3	N/D
M 3-8	358.2+04.2	17 24 52.152	-28 05 54.61	ext
B1 D	358.2-01.1	17 46 02.818	-31 03 39.33	N/D
SB 52	358.3-07.3	18 11 39.900	-34 00 21.99	N/D
JaSt 3	358.4+01.6	17 35 22.745	-29 22 17.40	N/D
NGC 6563	358.5-07.3	18 12 02.753	-33 52 07.14	ext
JaSt 4	358.6+01.7	17 35 37.47	-29 13 17.7	N/D
JaSt 58	358.6-01.1	17 46 52.20	-30 37 42.8	N/D
PHR1752-3116	358.7-02.5	17 52 36.5	-31 16 27	N/D
SB 53	358.7-05.1	18 03 28.532	-32 37 26.46	N/D
H 1-50	358.7-05.2	18 03 53.461	-32 41 42.15	N/D
JaSt 5	358.8+01.7	17 35 52.65	-28 58 25.7	N/D
Th 3-26	358.8+03.0	17 31 09.298	-28 14 50.43	ext

**Table 5.** continued.

name	PN G	$\alpha$ (2000)	$\delta$ (2000)	status
JaSt 9	359.0+01.1	17 38 45.91	-29 09 01.6	N/D
M 3-48	359.0-04.1	17 59 56.823	-31 54 27.46	ext
M 1-29	359.1-01.7	17 50 18.003	-30 34 54.90	ext
H 2-33	359.4-03.4	17 58 12.535	-31 08 05.99	ext
KnFs 3	359.7-04.4	18 02 52.931	-31 23 58.49	N/D
PPA1738-2800	359.9+01.8	17 38 11.8	-28 00 07	N/D

## Appendix A: Discussion about aperture

As we are dealing with extended sources, some special care had to be taken. Thus, we characterised the object sizes by means the Petrosian radius (Petrosian 1976; Yasuda et al. 2001) provided by CASU (see Table 4). However, the relation between a measured size and the real size of an extended nebula depends on the resolution/seeing versus actual size, and on the assumed geometry. There is a discussion on this in van Hoof (2000).

According to Fig. A.1 (upper panel), roughly 80% of PNe in our sample have a Petrosian radius less than 8 px, equivalent to 2.6''. In this sense, the magnitudes for our sample of PNe should be those of aperture-6 (= 2.83'') in the CASU catalogue.

In order to evaluate how important the differences between magnitudes obtained with an aperture 4 and 6 are, we assemble a histogram of  $\text{aperMag4} - \text{aperMag6}$  (Fig. A.2). Clearly, differences between both magnitudes are important. The tail towards brighter aperture-6 magnitudes may indicate the effect of extended sources and the presence of neighbour stars within the aperture. To evaluate this later hypothesis, we computed the number of stars that are closer than 2.6'' to each PNe. Surprisingly, about 70% of the sample do not have any contaminant star (Fig. A.3), pointing out that the differences should be due to other effects.

Alternatively, we analysed the sky subtraction performed by the CASU pipeline and found that the error introduced by this task is very significant. The weakest sources, as the PNe in our sample, are more affected by sky subtraction (see Fig. A.2). Also, we note that the magnitudes obtained with aperture-4 compare better with those of 2MASS (Fig. 2) than the aperture-6 ones, and the distribution of PNe in the  $J - H$  Vs.  $H - K_s$  diagram is more scattered.

Although it seems more appropriate to obtain the magnitudes with an aperture of 2.83'', increasing aperture implies increasing uncertainty in the magnitudes (due the sky subtraction), and the magnitudes obtained with larger aperture are affected by larger errors. In this sense, we demonstrate that the more accurate magnitudes are those computed with the CASU pipeline using the aperture of 1.41''.

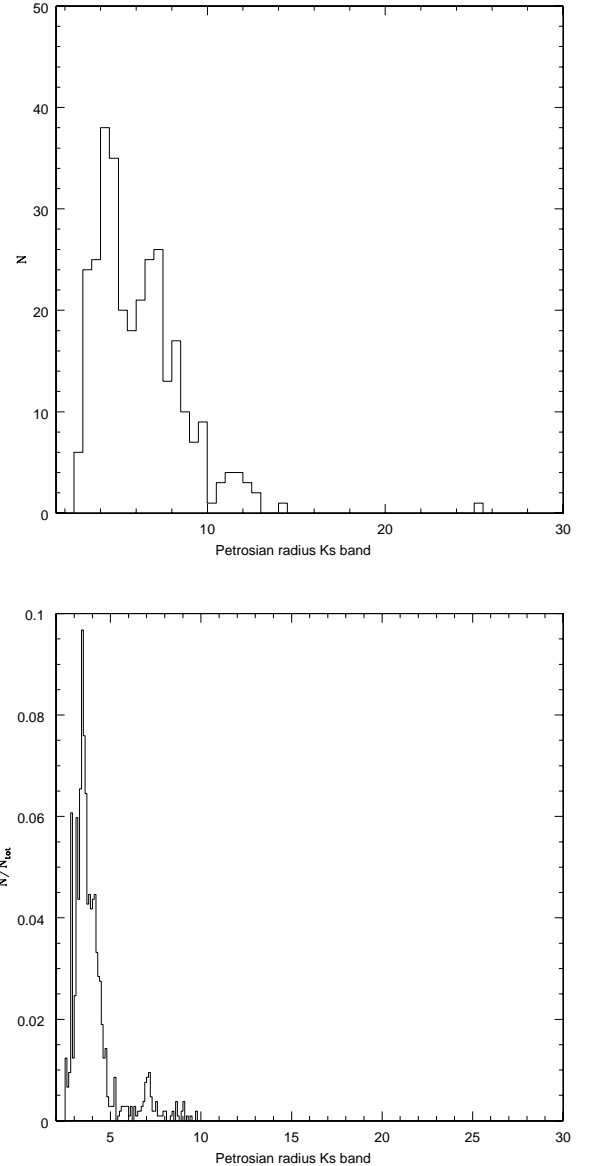


**Fig. A.1.** Distribution of Petrosian radii, in pixels. Upper panel, distribution for our sample of PNe (data from table 4). Lower panel, distribution for a sample of sources classified like stars by CASU.

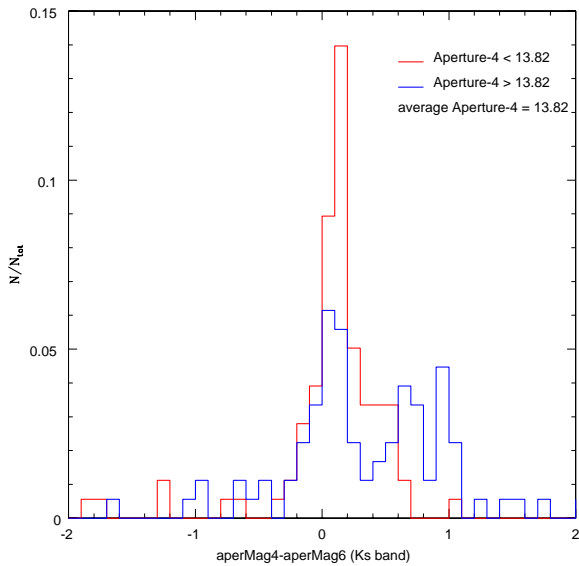


**Fig.A.2.** Comparison between magnitudes with aperture-6 (2.83'') and aperture-4 (1.41'') for our sample of PNe.

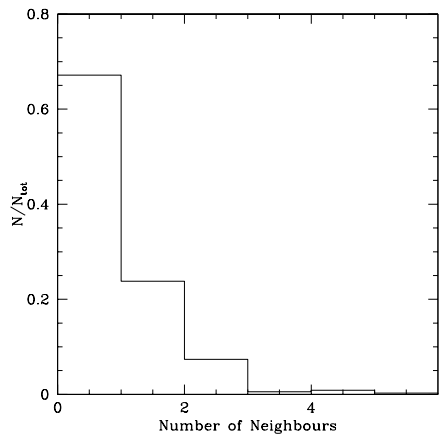


**Fig.A.3.** Distribution of number of contaminant stars around each PNe of our sample.

